PL-TR-94-2002 (I)

(2)

IONOSPHERIC PLASMA DRIFT AND STRUCTURE STUDIES AT HIGH AND MID-LATITUDES

Bodo W. Reinisch
James L. Scali
Claude Dozois
Geoffrey Crowley

University of Massachusetts Lowell
Center for Atmospheric Research
450 Aiken Street
Lowell, MA 01854

December 1993

Final Report

October 1990 - October 1993

Approved for public release; distribution unlimited

PHILLIPS LABORATORY
Directorate of Geophysics
Air Force Materiel Command
Hanscom Air Force Base, MA 01731-3010

"This technical report has been reviewed and is approved for publication."

B S Dandekar
Contract Manager

Edward Beyhorn
Maj Edward Berghorn, Chief
Ionospheric Application Branch

William K. Vickery
WILLIAM K. VICKERY, Director
Ionospheric Effects Division

This report has been reviewed by the ESC Public Affairs Office (PA) and is releasable to the National Technical Information Service (NTIS).

Qualified requestors may obtain additional copies from the Defense Technical Information Center (DTIC). All others should apply to the National Technical Information Service (NTIS).

If your address has changed, or if you wish to be removed from the mailing list, or if the addressee is no longer employed by your organization, please notify PL/TSI, 29 Randolph Road, Hanscom AFB, MA 01731-3010. This will assist us in maintaining a current mailing list.

Do not return copies of this report unless contractual obligations or notices on a specific document requires that it be returned.

REPORT DOCUMENTATION PAGE

Form Approved
OMB No. 0704-0188

1. AGENCY USE ONLY (Leave blank)	2. REPORT DATE	3. REPORT TYPE AND DATES COVERED
	December 1993	Final Report (Oct 1990 - Oct 1993)

4. TITLE AND SUBTITLE
Ionospheric Plasma Drift and Structure Studies at High and Mid-Latitudes

5. FUNDING NUMBERS
PE 62101F
PR 4643
TA 08
WU AU

Contract No.
F19628-90-K-0005

6. AUTHOR(S)
Bodo W. Reinisch, James L. Scali, Claude Dozois
Geoffrey Crowley

7. PERFORMING ORGANIZATION NAME(S) AND ADDRESS(ES)
University of Massachusetts Lowell
Center for Atmospheric Research
450 Aiken Street
Lowell, MA 01854

8. PERFORMING ORGANIZATION REPORT NUMBER

9. SPONSORING/MONITORING AGENCY NAME(S) AND ADDRESS(ES)
Phillips Laboratory
29 Randolph Road
Hanscom AFB, MA 01731-3010

Contract Monitor: Balkrishna S. Dandekar/GPIA

10. SPONSORING/MONITORING AGENCY REPORT NUMBER
PL-TR-94-2002 (I)

11. SUPPLEMENTARY NOTES

12a. DISTRIBUTION/AVAILABILITY STATEMENT
Approved for public release;
distribution unlimited

12b. DISTRIBUTION CODE

13. ABSTRACT (Maximum 200 words)

Ground-based observations of the high latitude ionosphere with Digisonde sounders at Qaanaaq, Sondrestrom, Goose Bay, Argentia and Millstone Hill provides a description of the patch structure and the convection pattern in the polar cap. Correlation analysis of observed F-region plasma drifts with the orientation of the interplanetary magnetic field (measured by IMP8) lead to a new technique of deducing the signs of Bz and By from the measured drifts. Real time calculation of the plasma drift was successfully introduced at one of the Digisonde stations (Sondrestrom) providing the possibility of determining the IMF components in real time. Analysis of mid-latitude trough observations shows large westward velocities in the trough region. Digisonde data from Qaanaaq and DMSP F8 and F9 satellite data showed the development of the ionospheric polar hole.

14. SUBJECT TERMS	15. NUMBER OF PAGES
High Latitude Ionosphere, Polar Cap, Digisonde, Real-Time Drift, Trough, Polar Hole	70
	16. PRICE CODE

17. SECURITY CLASSIFICATION OF REPORT	18. SECURITY CLASSIFICATION OF THIS PAGE	19. SECURITY CLASSIFICATION OF ABSTRACT	20. LIMITATION OF ABSTRACT
Unclassified	Unclassified	Unclassified	SAR

Table of Contents

List of Illustrations

List of Illustrations (Continued)

List of Illustrations (Concluded)

List of Tables

1. INTRODUCTION

The understanding of the upper atmosphere dynamics is essential in order to determine the likely impact changes in the ionospheric structure have on Air Force radio-wave communication systems. This final report summarizes the results and achievements in this area made during the project contract covering the period from October 1989 to October 1993.

Data from different instruments were used in the study of the high latitude ionosphere, including the Incoherent Scattering Radar (ISR) located at Sondrestrom (Greenland), the Defense Meteorological Satellite Program (DMSP) F8 and F9 satellites, and the digital ionosondes located at Qaanaaq, Sondrestrom, Goose Bay, Argentia and Millstone Hill. The key instrument for our studies was the Digisonde (Reinisch et al., 1991), and its militzrized equivalent the AN/FMQ-12, Digital Ionospheric Sounding System (DISS), both of which are advanced digital ionosondes developed by UMLCAR. Since this instrument is a low cost and low maintenance device, which continuously supplies the electron concentration profiles and the ionospheric drift velocities in real time, it is ideally suited for the monitoring of the polar ionosphere on a continuous basis. Use of the various instruments listed allows snapshots of the high-latitude convection patterns to be obtained; however, due to site and instrument limitations, collecting a continuous set of data from the ISR and DMSP satellites is not possible.

Comparison of data types from the ISR and DMSP satellites with the Digisondes provides verification of the high quality of data being recorded by the Digisondes on a routine basis. Therefore in this project, data collected by the Digisonde were mainly used in the interpretation of the geophysics of the high latitude ionosphere.

Phillips Laboratory and the Air Weather Service currently operate a network of four Digisondes, DISS, which together with the UMass Lowell Digisonde at Millstone Hill, cover a range from the mid-latitude to the central polar cap. The different sites provided high quality data sets on a routine basis. An upgrade of the DISS at Sondrestrom has made it possible to not only calculate the electron density profiles, but also the drift velocities in real time. The results from the polar cap cusp and auroral stations show the potential of the Digisonde network to map out real time convection patterns and specify important parameters needed as input from geophysical models.

2. SPECIFIC PROJECT GOALS

A number of project goals were specified under this contract. While the goals did include development of special hardware and software features for the Digisonde systems, the main emphasis was the geophysical interpretation of the results obtained by the Digisondes at the four high latitude stations. To briefly summarize the original intent of this project, the following list is supplied as a guideline.

2.1 Hardware/Software Development

1. Update, test and calibrate the AWS DISS Digisonde at Sondrestrom.
2. Develop and install an Onsite Digisonde Drift Analysis "ODDA" package at Sondrestrom for the real time calculation of drift velocity vectors.
3. Develop an Onsite Quality Control "OQC" package for the drift data being recorded.

2.2 Geophysical Research

1. Investigate the phenomena of Patch movements across the polar cap.
   - What is the actual mechanism of patch generation?
   - What controls patch amplitudes (with respect to background ratio in Ne)?

2. Systematically study the F-Region Polar Cap convection pattern.
   - How does this convection pattern change under different IMF conditions?
   - Is it possible to determine the convection patterns from a limited number of ground stations?
   - How do the Digisonde drift velocities compare with velocities measured by other instruments?
   - Importance of convection in the Summer Polar Cap?
   - Are the estimated convection patterns useful drivers for more involved ionospheric models?

3. Investigate the characteristics of the Mid-latitude Trough.
   - What is the relationship between convection and trough generation?
   - How does the F-region trough affect oblique propagation?

4. Develop a comprehensive drift data base.

3. HARDWARE / SOFTWARE UPGRADES

The AWS DISS installed at Sondrestrom in 1989 has been upgraded to run new drift modes and operate the Automatic Real Time Ionogram Scaler with True Height (ARTIST3/ODDA) software package.

3.1 Processor Upgrades

The Digisonde Processor at Sondrestrom has been upgraded to run the fast drift modes, the 4O-4X polarization modes and improved CPU I/O access by using "Direct Communication". A detailed description of these improvements was given in Quarterly Report #1, relevant sections of which are reproduced in Appendix A. All new drift modes were tested and are now operational at the station.

3.2 Computer Upgrade

The original IBM PC/AT was replaced by a 386 ARTIST3/ODDA configuration computer. Figure 1 displays the basic system requirements. In order to run the new ARTIST3/ODDA package, a 386 PC running at 25 MHz or greater is needed. The drift data is now recorded to 150MByte 1/4 inch cartridges which are more compact and easier to handle than the older 9-track tapes. The cartridge drives are contained within the controlling PC computer and can be changed quickly if problems exist. In the period after installation of the ARTIST3/ODDA system in July 1992 the computer configuration has performed reliably and it is strongly recommended that other systems be upgraded to this new configuration.

3.3 Software Upgrade

The new ARTIST3/ODDA software package has been installed in Sondrestrom. The package contains: improved I/O communications with the Digisonde Processor, a backup TSR program to handle the automatic transfer of ionosonde data to cartridge tape, an improved ARTIST program with the latest profile inversion techniques, a quality control package to assess the performance of the Digisonde system (Scali 1993) and a real time calculation of the drift velocity vectors. Details of the ODDA development were documented in all quarterly reports and is not further discussed.

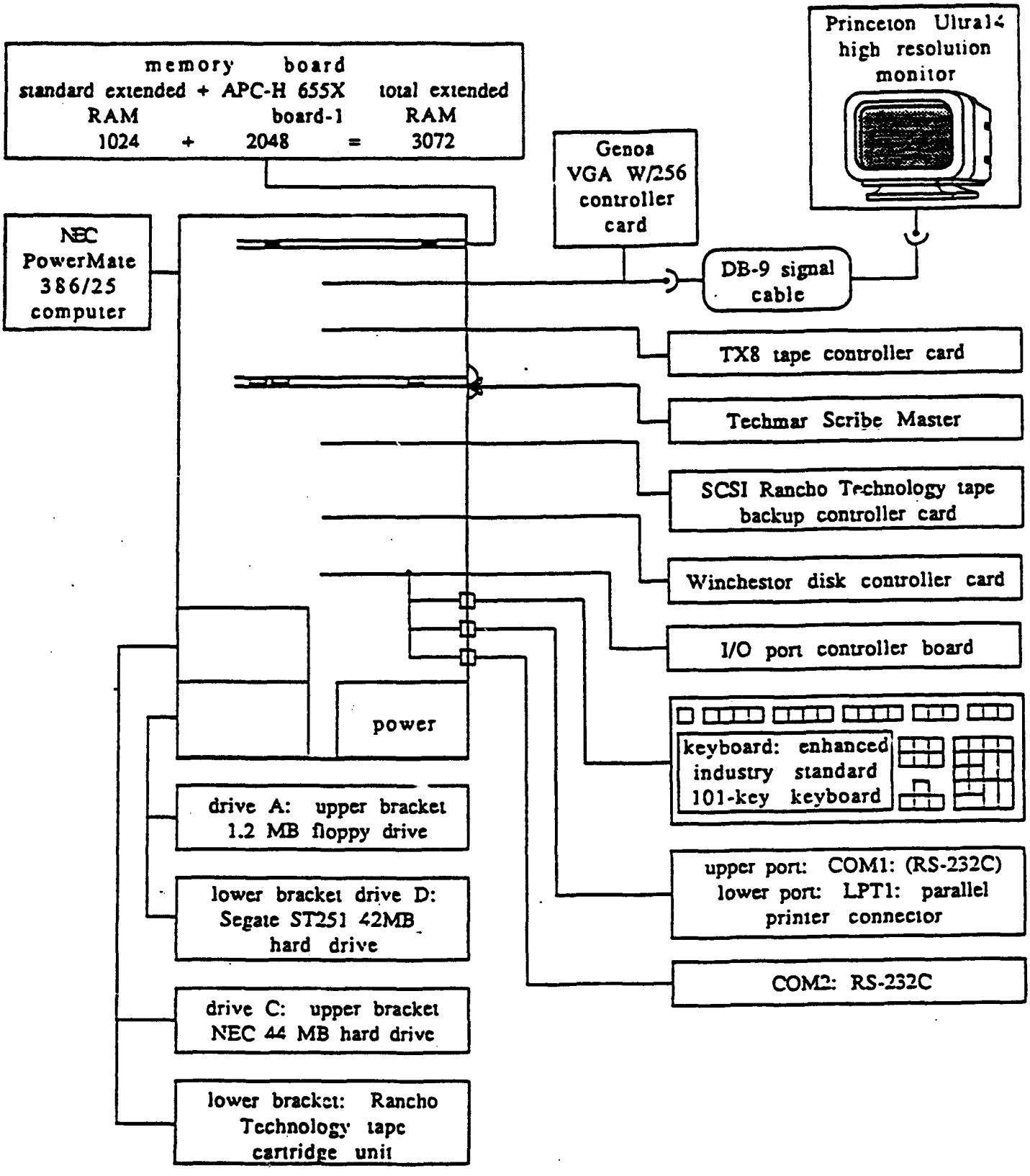

Figure 1. ARTIST3/ODDA Configuration.

4. GEOPHYSICAL RESEARCH

Digisonde observations at Qaanaaq, Sondrestrom, Goose Bay and Argentia have been used to obtain a systematic study of the polar cap F-region plasma convection. The next sections summarize the important discoveries made by these analyses and their significance to specific ionospheric phenomena. The database collection has been discussed in each Quarterly Report under the "Development in Drift Data Processing by Station" section. The availability of data recorded and processed at each station is given in Tables 1 to 4.

Most of the data recorded during the contract period have been processed. However, due to different campaigns, instrument down times, availability of computer storage space, and data processing improvements it was not possible to complete the processing of all the drift data. The large volume of drift data being collected suggests that the ODDA real time system, like the one installed in Sondrestrom, should be implemented at each station so that skymaps and velocities are calculated in real time, thus cutting post processing time to a minimum.

The following sections outline the main achievements in the understanding of the geophysics of the polar cap F-region dynamics studied under this project.

4.1 Patch formation

A summary of the polar cap patch characteristics and their seasonal behavior was given by Buchau and Reinisch (1991). Current theories of polar patch generation suggest that ionospheric plasma is transported into the polar cap from sub-auroral region (sub-cusp) in the noon sector, under Bz southward conditions (Anderson et al., 1988). Multistation Digisonde drift observations clearly support the two-cell convection pattern for negative Bz as illustrated in Figure 2, which shows a polar plot of the horizontal drift vector measured at Goose Bay, Sondrestrom and Qaanaaq during 24 hours. The vectors are plotted in corrected geomagnetic latitude and local time. The data have been smoothed by a weighted nine point function to show the main features.

Table 1. Processed Argentia Drift Data

Station: Argentia
Latitude: 47.3N
Longitude: 306.0E

Period Covered	Raw Drift Data Collected (%)	Skymap Data Processed (%)	Velocity Data Processed (%)
Oct - Dec 1989	78.0	100	100
Jan - Dec 1990	37.3	100	100
Jan - Dec 1991	49.9	100	100
Jan - Dec 1992	15.6	77.2	90.9
Jan - Oct 1993	2.3	100	100

Table 2. Processed Goose Bay Drift Data

Station: Goose Bay
Latitude: 53.3N
Longitude: 299.2E

Period Covered	Raw Drift Data Collected (%)	Skymap Data Processed (%)	Velocity Data Processed (%)
Oct - Dec 1989	85.9	100	94.9
Jan - Dec 1990	81.6	100	95.6
Jan - Dec 1991	94.8	100	99.4
Jan - Dec 1992	86.8	96.5	98.7
Jan - Oct 1993	37.5	96.5	100

Table 3. Processed Sondrestrom Drift Data

Station: Sondrestrom
Latitude: 66.9N
Longitude: 309.05E

Period Covered	Raw Drift Data Collected (%)	Skymap Data Processed (%)	Velocity Data Processed (%)
Oct - Dec 1989	76.1	100	94.3
Jan - Dec 1990	35.6	100	100
Jan - Dec 1991	61.4	100	99.5
Jan - May 1992	19.9	100	97.0
June 1992 - Oct 1993	ODDA was operational, and since skymaps and velocity files were generated at the station in real time, no post-processing of the data was required.		

Table 4. Processed Qaanaaq Bay Drift Data

Station: Qaanaaq
Latitude: 77.5N
Longitude: 290.08E

Period Covered	Raw Drift Data Collected (%)	Skymap Data Processed (%)	Velocity Data Processed (%)
Oct - Dec 1989	100	100	100
Jan - Dec 1990	97.5	100	100
Jan - Dec 1991	86.9	100	100
Jan - Dec 1992	98.5	73.7	100
Jan - Oct 1993	34.9	0	0

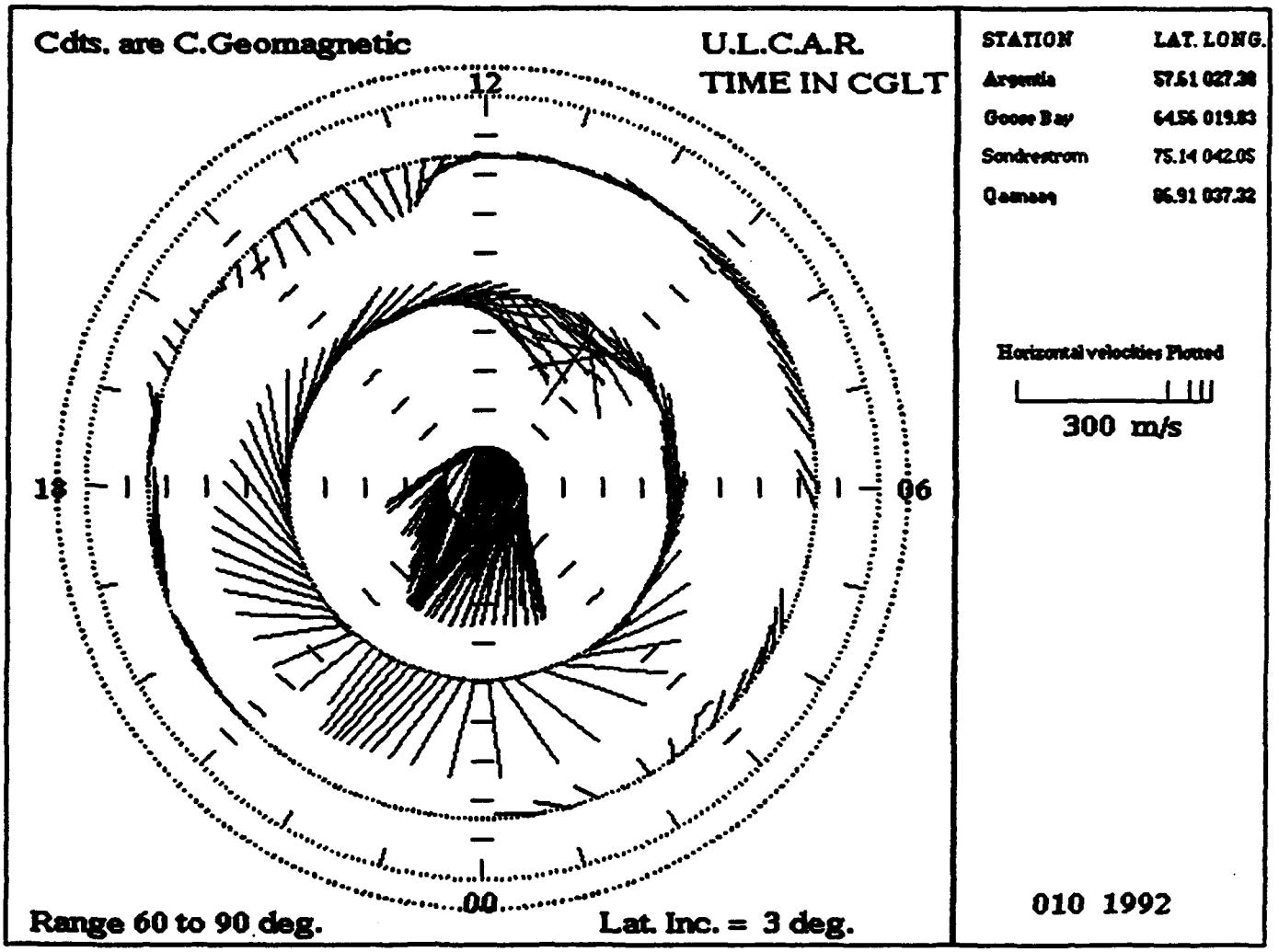

Figure 2. Polar plot of Digisonde calculated horizontal velocity component. Measurements made at Qaanaaq (Greenland). Sondrestrom (Greenland) and Goose Bay.

The data shown in Figure 2 was recorded on 10 January 1992 during which the Bz was consistently southward. Qaanaaq (87° CGL) clearly displays anti-sunward motion through the entire day, while Sondrestrom (76° CGL) outlines a two cell convection pattern where the cusp is located at approximately 11MLT and the Harang discontinuity at magnetic midnight. The convection at the lower latitude of Goose Bay (65° CGL) does not display any close correlation to the higher latitude stations, since on this night Goose Bay was located close to the equatorial side of the mid-latitude trough.

Considering the convection pattern observed at Sondrestrom, patches of plasma peel off the reservoir of the sunlit ionization region at sub-cusp latitudes and flow into and across the dark polar cap [Buchau and Reinisch, 1991]. These patches are observed at Qaanaaq as enhanced electron densities as shown in Figure 3, showing the diurnal variations in foF2 for three consecutive days from 6 to 8 January 1992. On all days distinct enhancements are observed after 17UT. During this time foF2 values increase by as much as 5MHz above the background ionization levels. While the drift and electron density measurements made at Qaanaaq, Sondrestrom and Goose Bay have allowed a better understanding into the transport of these patches over the polar cap, the actual mechanism responsible for the peeling off of these patches from the sub-cusp reservoir is still unclear. From the high velocities observed in the cusp region over Sondrestrom in Figure 2, one could argue that a vortex (Valedares, personal communication) is set up that literally pulls the sub-cusp plasma into the polar anti-sunward flow. More analysis is required before a complete understanding of the patch generation processes can be attained.

4.2 Polar Convection Monitoring (PCM) Study

The analysis of the interconnection of the IMF with the polar cap convection pattern began in Quarterly report #6 under the section entitled "Study of the Polar Cap Convection for Bz Northward". While only the convection patterns for when Bz>0 (northwards) were discussed, a great deal of insight into the behavior of the convection pattern for Bz<0 was also obtained. The main objectives in this study were to use a network of ground-based observation stations (such as a Digisonde

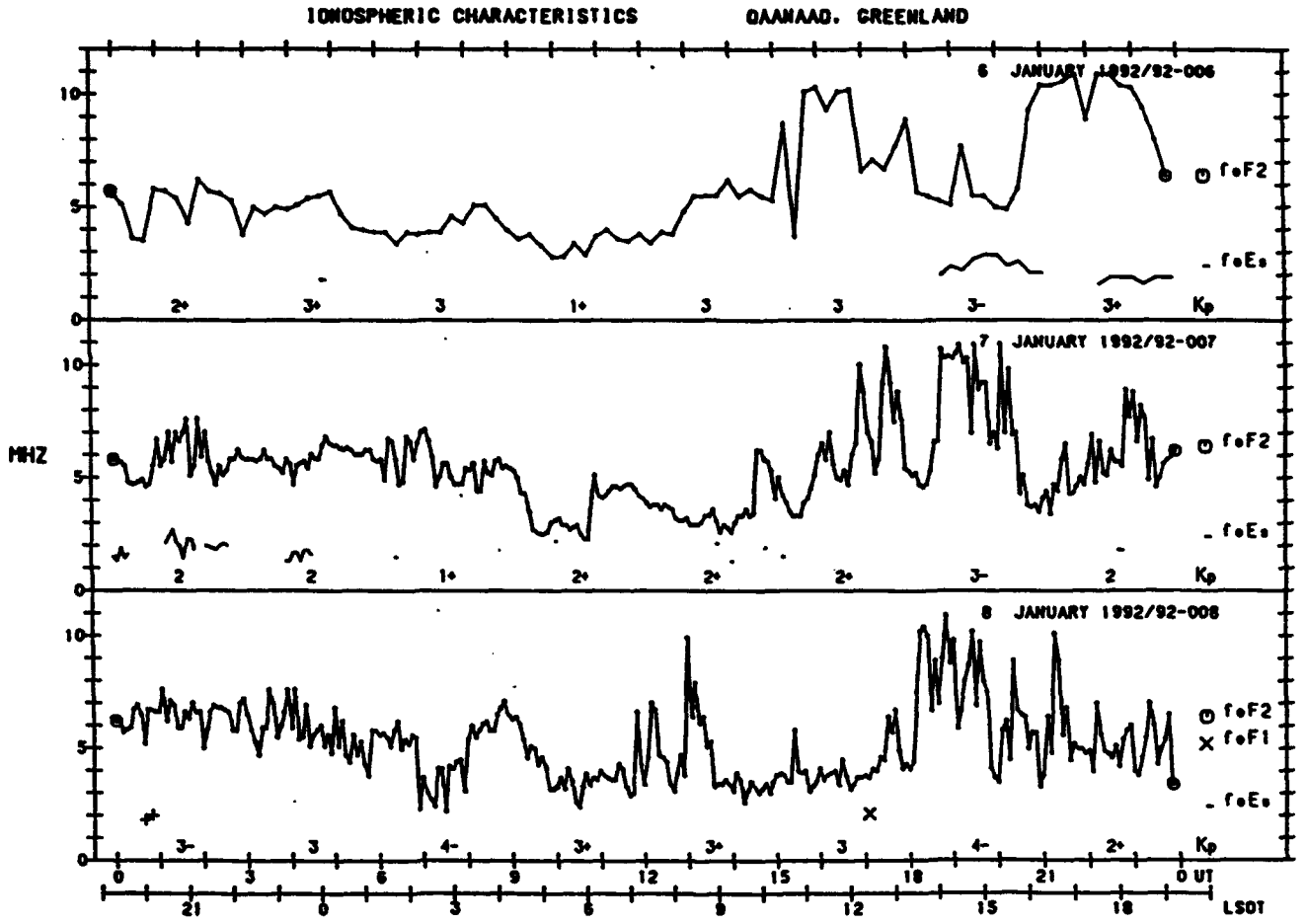

Figure 3. Diurnal variation of foF2 measured at Qaanaaq from 6 to 8 January 1992.

network) in order to specify, as a minimum, the orientation of the IMF (sign of Bz and By components), the position of the dayside cusp region and the nighttime Harang discontinuity. These inputs are essential for empirical and physical models in order to specify the convection pattern.

A review of the theory and assessment of the prediction of the IMF Bz and By components from drift measurements for only one Digisonde station is given by Scali et al. (1993). At high latitudes the magnetospheric solar wind induced electric fields map into the ionosphere along the open and closed field lines driving the ExB drifts. For the two-cell convection during Bz<0 conditions the Digisondes measure consistently high horizontal velocities in the polar cap (Cannon et al., 1992). For Bz>0, from this work (Crowley et al, 1993; Cannon et al., 1993), previous theoretical understanding and satellite observations (Heelis et al., 1986), the general consensus is that a four cell convection system exists and the horizontal velocities are observed to be appreciable smaller.

An example of the Bz control on the convection pattern is shown in Figure 4, displaying drift data measured at Qaanaaq on days 91099 to 91101. The magnitude of the horizontal velocity and vertical velocity as well as the azimuthal direction of the horizontal velocity are given in this plot. On day 99 when Bz<0 (Figure 5), the plasma flow is strictly anti-sunward. On day 100 after 12UT when Bz is northward (Figure 6), sunward motion is observed, and the lower horizontal velocity magnitudes are small (150m/s). These two distinct and simple characteristics of the behavior of the convection during changes in the IMF Bz sign suggest that the drift velocities at Qaanaaq may be used to determine the orientation of the IMF Bz component.

From the statistical analysis of Qaanaaq drift data it is possible to define the convection patterns observed for different IMF conditions. Conversely understanding more about the physics of the F-region dynamics allows the orientations of the IMF Bz and By components to be inferred from the Digisonde drift measurements. The statistical analysis showed that while the IMF Bz component controls the location of the merging magnetic field lines and so determines the coarse structure of the convection pattern (i.e. either a two cell or a four cell), the By component controls the shape of the flow cells.

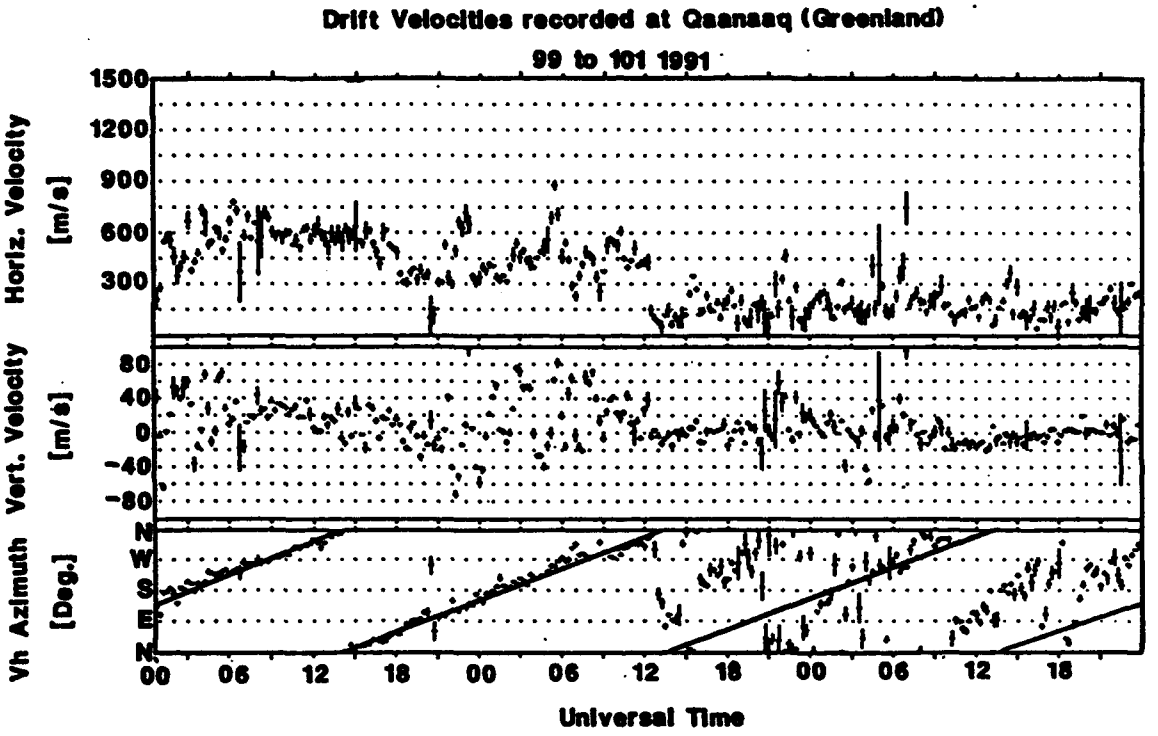

Figure 4. Digisonde drift velocities measured at Qaanaaq from 9 to 11 April 1991. Continuous line in Az represents modeled anti-sunward direction.

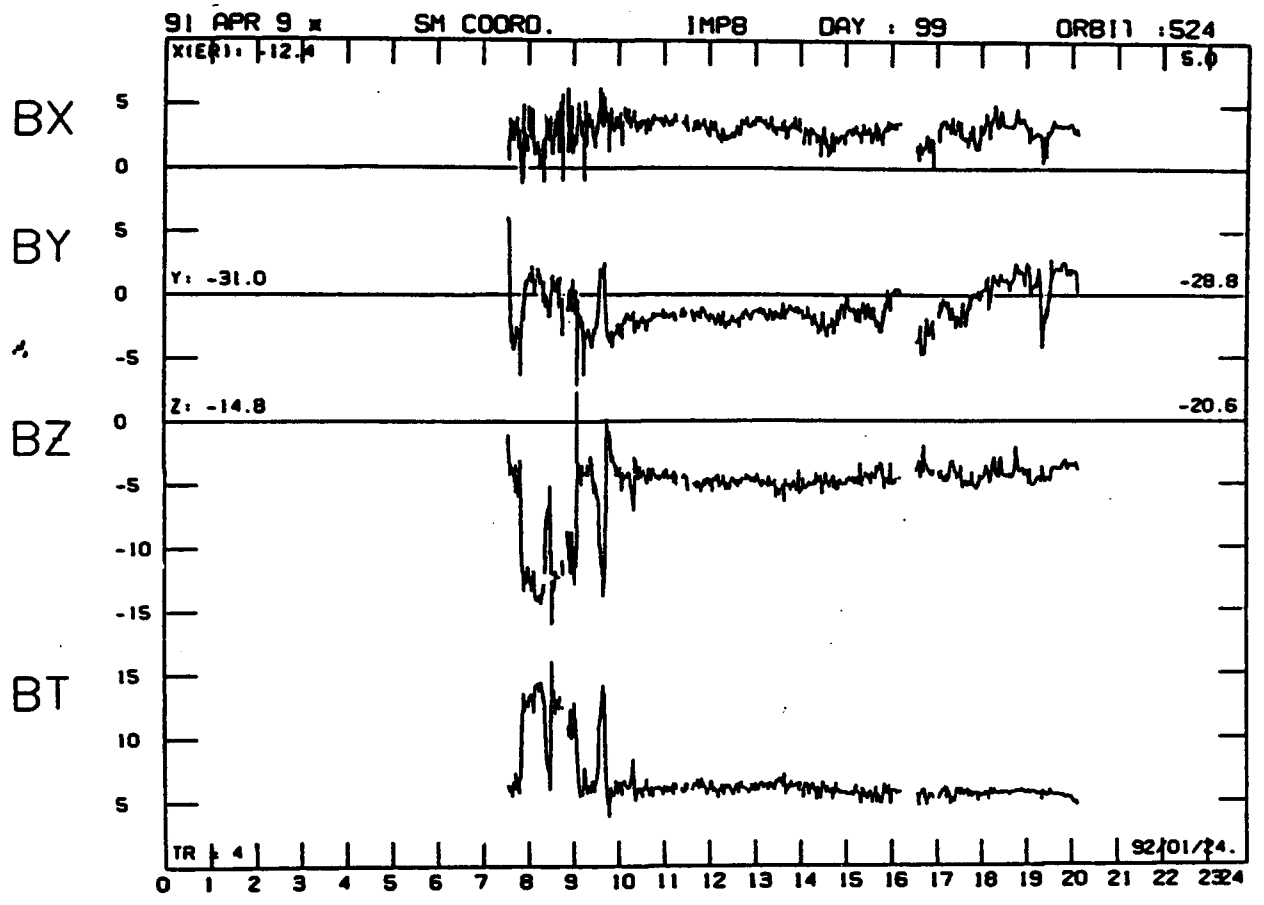

Figure 5. IMP8 satellite IMF data for most of day on 9 April 1991, Bz<0.

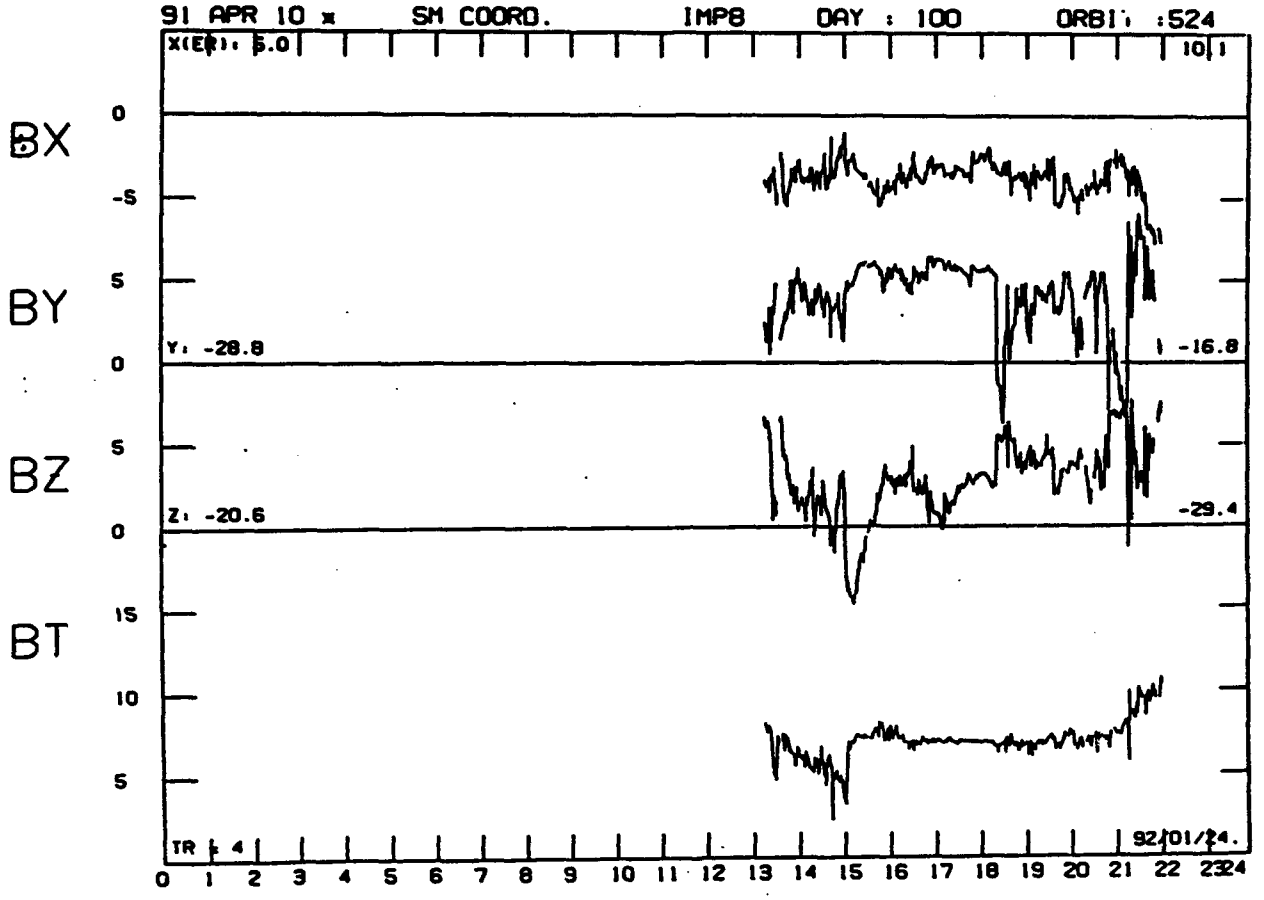

Figure 6. **IMP8 satellite IMF data. On 10 April 1991 Bz is northward (>0) after 12 UT.**

Figure 7 displays the orientation of two cell modeled convection patterns calculated by Heppner and Maynard [1987] for Bz<0 and different By conditions, together with the flow data measured by the Digisonde at Qaanaaq (Cannon et al., 1991). The figure shows that when By<0 the dawn cell expands and the velocities in the polar region have directions slightly east of anti-sunward. When By>0 the dusk cell dominates and the velocities are directed west of anti-sunward. Both features are verified by the drift measurements made at Qaanaaq. When Bz>0 the convection patterns become more complicated. Figure 8 displays the vector averaged flow patterns and estimated equipotential lines derived from Qaanaaq drift observations (Crowley et al., 1993). When By > 0, a clockwise rotating cell in the dayside is produced moving ionization from dawn to dusk in a sunward direction. When By≈0 (Bz dominant), a four cell pattern is suggested by the observations with the two dayside cells located symmetrically around noon. When By<0, a dawn counterclockwise rotating cell is dominant in the dayside.

Based on the above discussions, preliminary techniques were developed to determine the sign of the IMF Bz and By components from Digisonde drift measurements made at a single station (Qaanaaq). The methods proved to be quite reliable as shown in Figure 9, displaying a comparison between the deduced Bz and By orientations and the Bz and By values measured by the IMP8 satellite. The deduced Bz and By orientations are represented by the dashed line. Although the satellite data is limited, the overall comparison is good. The Bz component (top graph) reverses around 19UT, however, the velocity data does not show a change in the convection pattern until 20UT after which time the method determines the correct Bz sign. Note that the dashed lines represents a quality factor indicating the confidence in the deduced sign of Bz or By, and it is not a measure of Bz and By field magnitudes. The deduced By orientations (bottom graph) compare well with the By variation measured by the satellite.

Testing these methods over an entire year for all times of the day, the results show that the sign of the IMF Bz and By components can be determined accurately from the Qaanaaq drift data 60 to 70% of the time. Considering that this is a single station determination and that the convection patterns are generally well defined in certain time sectors, the ability of this scheme to offer this degree of accuracy is important. Folding in other stations such as Sondrestrom, which we have already observed in

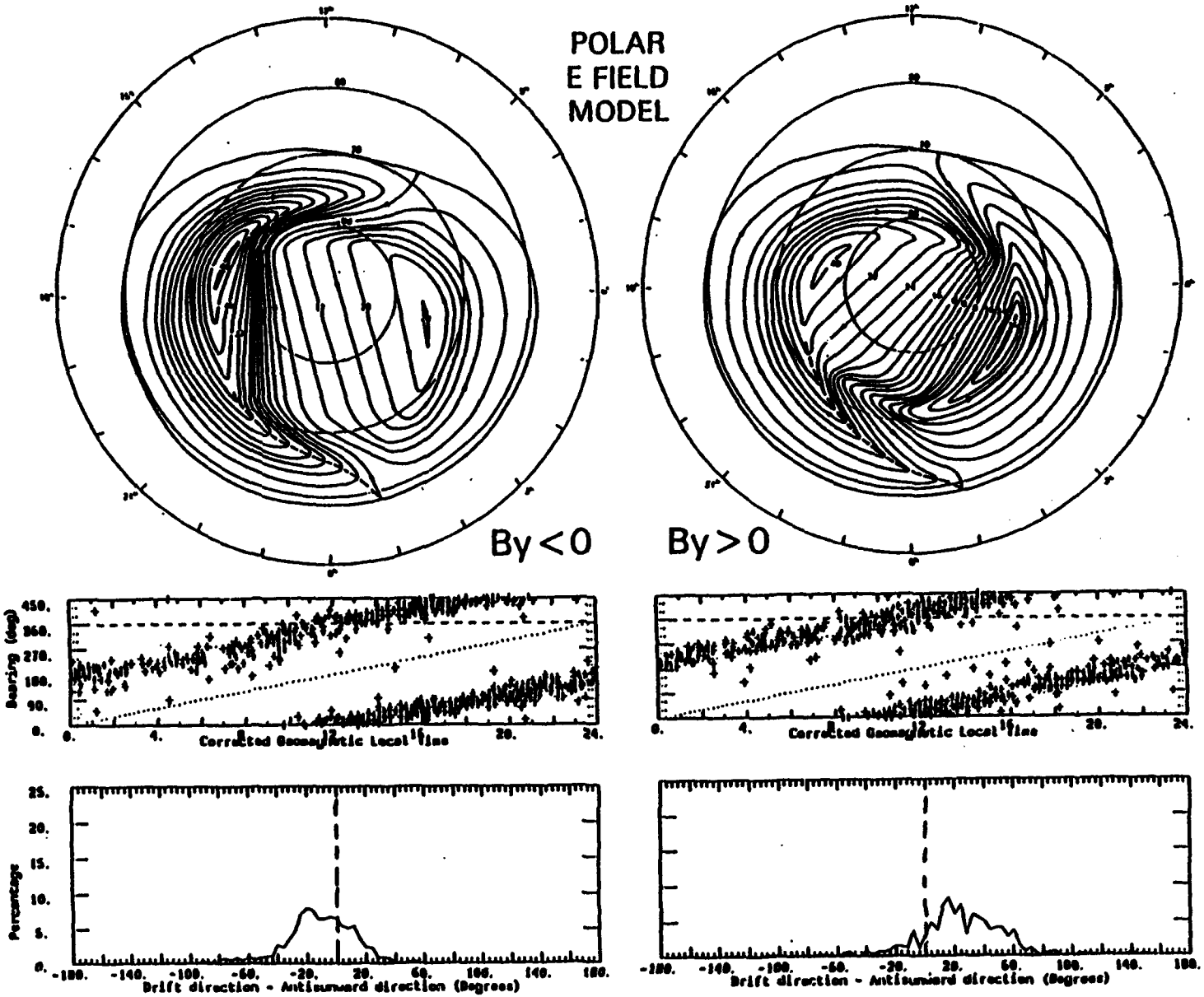

Figure 7. Orientation of two cell modeled convection patterns taken from Heppner and Maynard (1987) for Bz<0 and different By conditions. Below are the measured Digisonde horizontal angular velocity component averaged over data collected in 1989. The distribution of the deviation of the horizontal drift angle with respect to anti-sunward direction is also supplied.

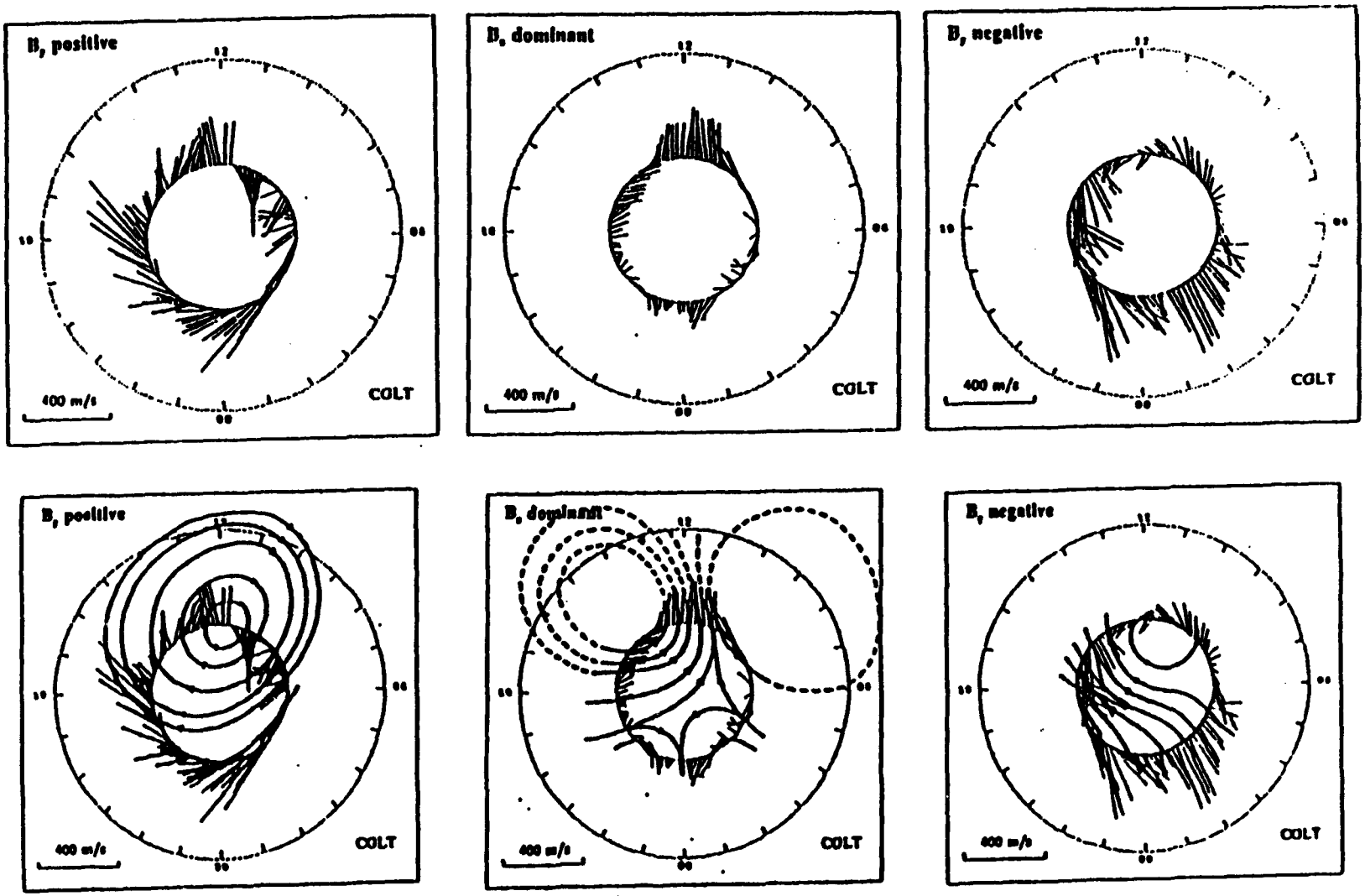

Figure 8. Vector averaged drift flow patterns and estimated equipotential lines.

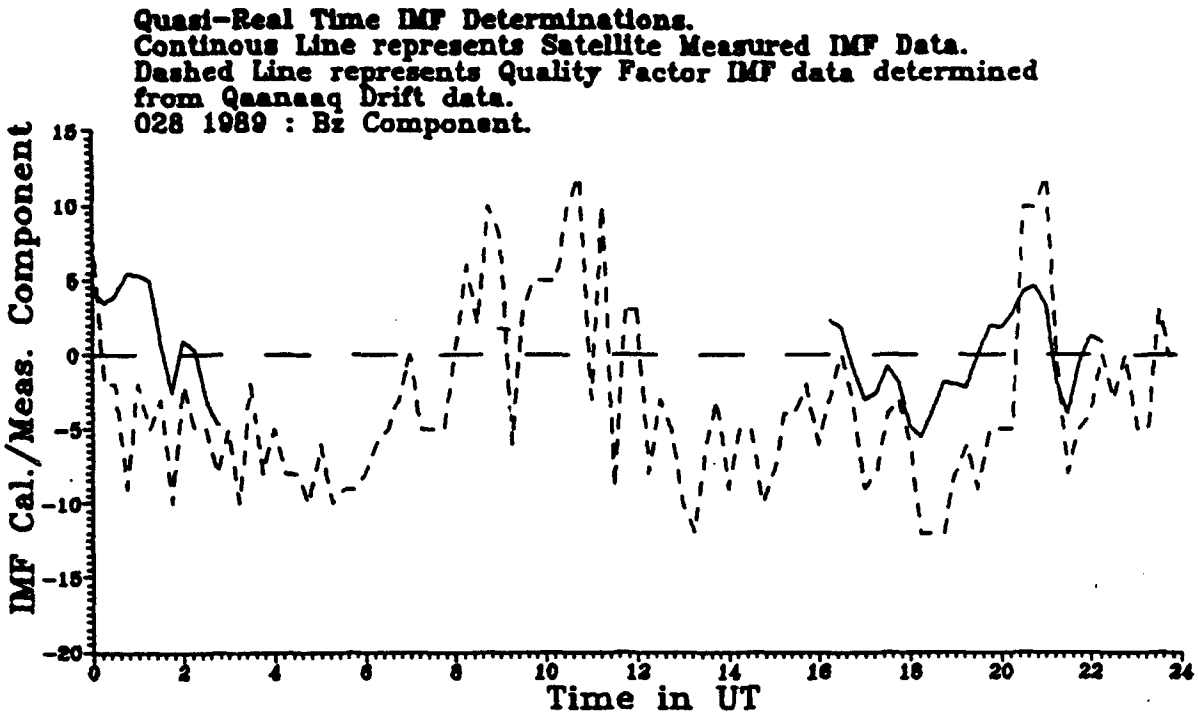

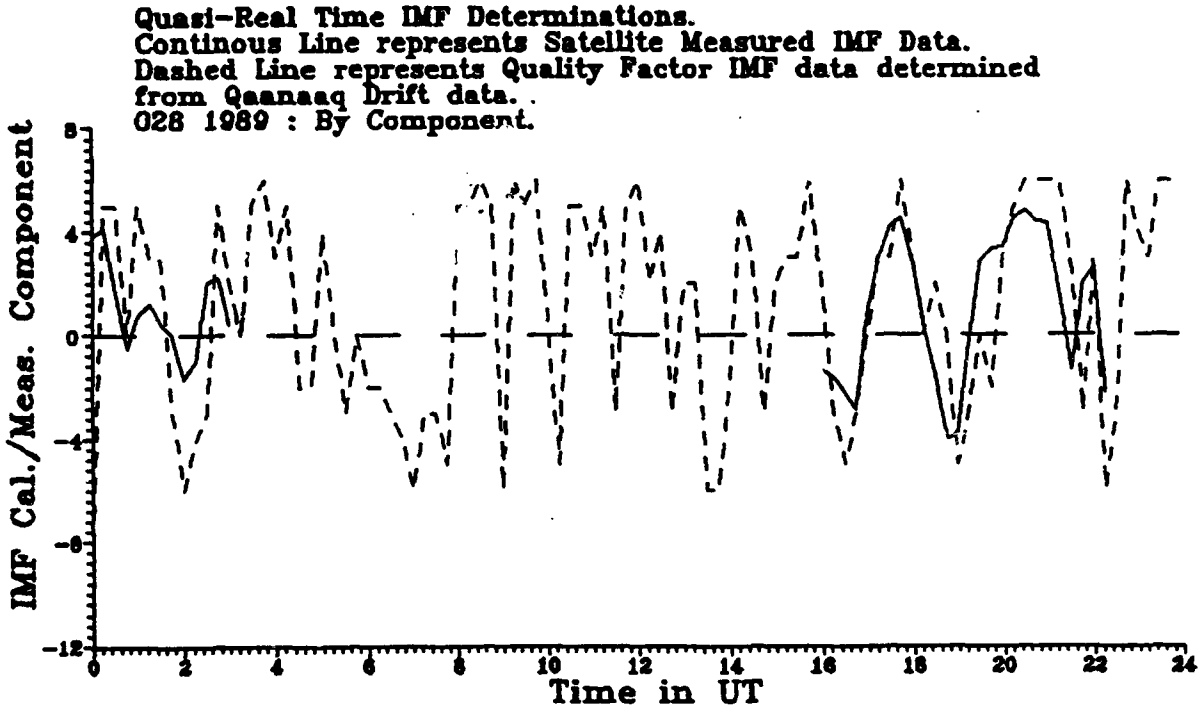

Figure 9. Satellite measured and Digisonde calculated IMF orientations.
(a) Represents results for sign of Bz.
(b) Shows comparison results for sign of By.

Figure 2 to clearly show the cusp and Harang discontinuity regions, will greatly improve the reliability in the determination of the Bz and By orientations and make the Digisonde network a viable asset to the continuous monitoring of the convection in the polar region. As an example of the coverage offered by the four stations considered under this contract, Figure 10 shows the polar plot of the horizontal velocities measured at Argentia, Goose Bay, Sondrestrom and Qaanaaq.

Figure 10 displays drift data measured on days 89192 and 90353 at four high latitude stations. Both days were quiet geo-magnetically with Sums of Kp less than 8. On day 89192, the IMF Bz component generally remained less than or equal to zero. The anti-sunward flow of ionization over Qaanaaq is observed. At Sondrestrom the two cell convection, daytime cusp and Harang discontinuity are observed. On day 90353, however, Bz was positive most of the day. The characteristic sunward flow in the dawn sector is observed, however, the identification of a daytime cusp in the Sondrestrom data becomes obscured which is to be expected from the results presented above, suggesting a more complex three or four cell structure.

The lower latitude stations (Goose Bay and Argentia) are not influenced by the polar cap convection system, but tend to display velocities due to a more localized phenomena, as is suggested by the good correlation between these stations at certain times of the day. In general, the velocities measured at these stations during the Winter months differ considerably from those observed during the Summer months. In Northern Hemisphere Summer (represented here by day 89192) ionization tends to flow predominantly in a North to North-East direction. While in Northern Hemisphere Winter (represented by day 90353) the velocities are predominantly in the South to South-East direction in the daytime sector and in the South to South-West direction in the nighttime sector. This effect is especially evident in the velocity vectors displayed for Argentia in Figure 10. As yet an explanation for this observed difference in the Summer and Winter velocities for these high latitude stations has not been investigated. The seasonal variation at first suggests that neutral winds may be causing this effect, however, the magnitudes of the dayside velocity vectors are much larger than would be expected due to the contribution of neutral winds alone.

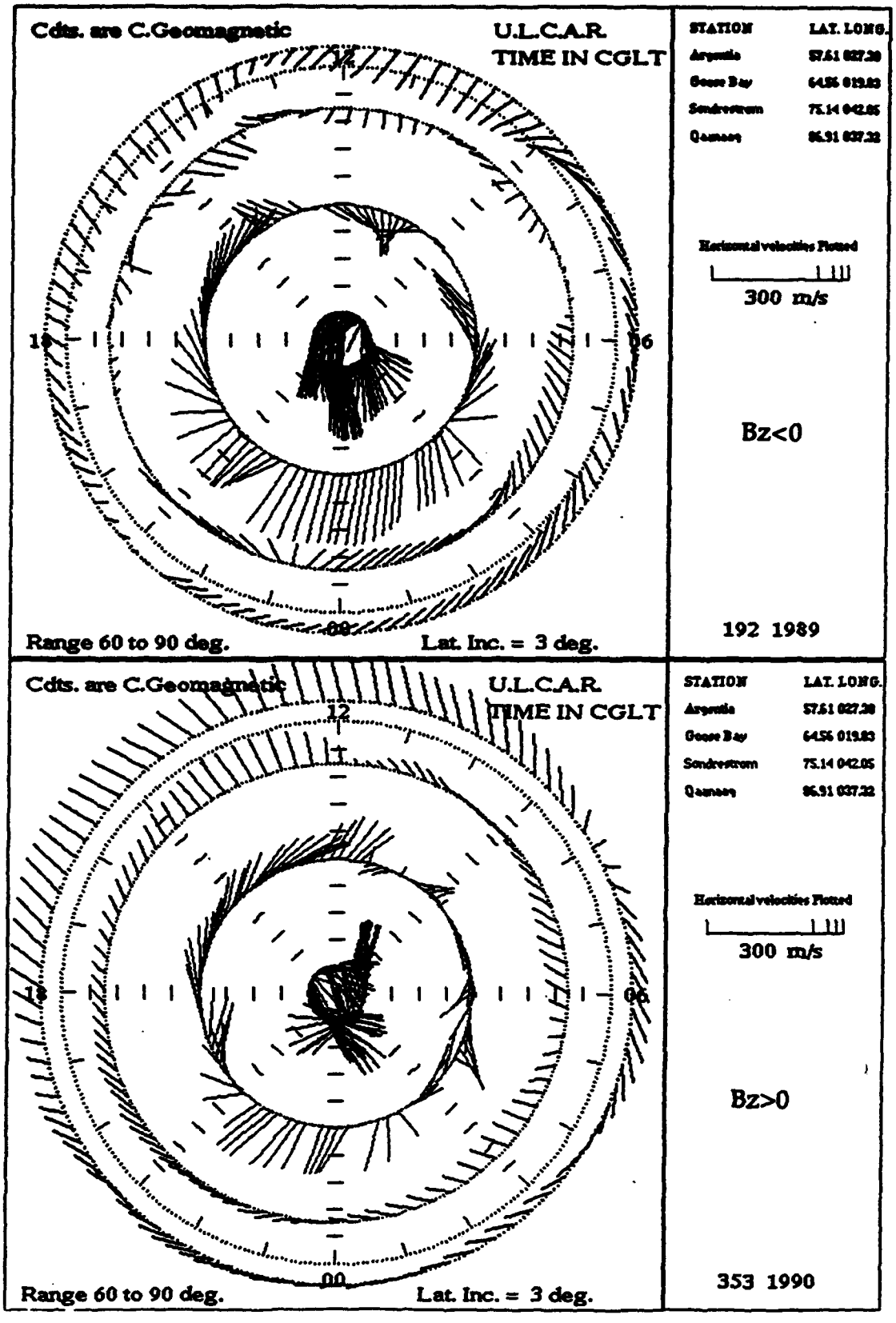

Figure 10. Polar plot of Digisonde horizontal velocities measured at Argentia, Goose Bay, Sondrestrom and Qaanaaq, 11 July 1989.

4.3 Trough Formation

The importance of identifying what type of trough is being observed is crucial for comparisons to other databases. Currently four possible trough categories exist; the main trough (or mid-latitudes trough), the high latitudes trough (or the Ionospheric Polar hole), the light-ion trough and the daytime trough. A good description of these various types and common theories for their formation was given by Scali (1992). In this study of trough formation two separate phenomena, the ionospheric polar hole and the mid-latitude trough are briefly discussed. The results of these studies have been published (Crowley et al., 1993; Scali and Reinisch, 1993).

4.3.1 The Ionospheric Polar Hole

The polar hole is a region of depleted F-region electron density in the polar cap. The polar hole discussed here is generally observed between 70 - 80 degree invariant latitudes and is restricted to the nightside polar cap. Under magnetically quiet conditions, polar holes are thought to form in regions where no solar illumination or ionizing particle precipitation occurs and the convection of plasma across this region is slow. Since the plasma is confined to the dark polar cap for a longer period of time, normal recombination processes deplete the electron concentration to low levels. This theory of the polar hole formation is well accepted and results obtained under this contract tend to confirm this process.

During the Geospace Environment Modeling (GEM) Pilot Program campaign of 16 January 1990, the spatial and temporal development of a polar hole was monitored by the DMSP F8 and F9 satellites, the Digisonde at Qaanaaq and the 250 MHz scintillation receiver at Thule, Greenland. The polar hole observed was relatively restricted in area and the electron concentration depletion was very small.

Figure 11 (Crowley et al., 1993) shows the DMSP F8 measurements made between 0135 to 0152UT on January 16, 1990. This set of graphs display the ion concentration, horizontal and vertical velocities, as well as the electron and ion precipitation. In this figure two trough regions are identified. The smaller trough observed at 0151UT is the mid-latitude trough, while the larger trough located between 0144 and 0146UT is the polar hole. It is important to observe the sharper sides of the polar

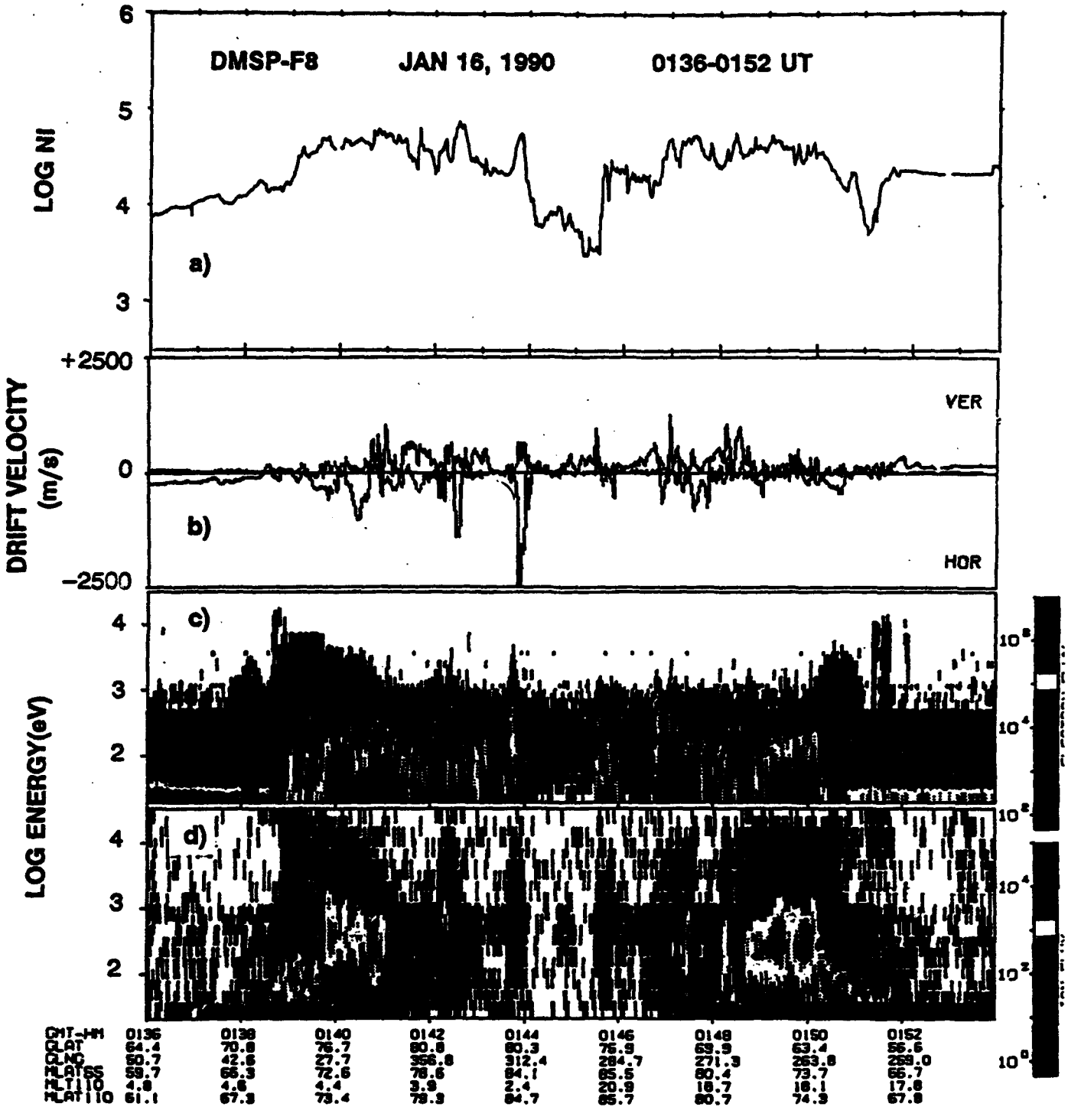

Figure 11. DMSP F8 measurements of the (a) ion concentration; (b) the horizontal and vertical velocity; (c) the electron precipitation and (d) the ion precipitation, showing an ionization polar hole event (Crowley et al., 1993).

hole as compared to the mid-latitude trough, and that the polar hole is located in a region where there is a minimum in electron and ion precipitation. Precipitation in the polar cap maintains ionization levels in two ways. First, precipitation leads directly to ion production and second, the particles heat the F-region plasma leading to an increased plasma scale height. Removal of the precipitating ions and electrons will deplete electron densities via recombination processes.

The sharpness of the edges of the polar hole can also be observed in foF2 values obtained from the Digisonde at Qaanaaq as shown in Figure 12 (Crowley et al., 1993). In this figure, both the foF2 and hmF2 parameters are plotted from 16UT on January 15 to 16UT on January 16 1990. Note that the electron concentrations at the sides of the polar hole are smaller than in the middle. Figure 13 (Crowley et al., 1993) shows the development of the polar hole as a function of time. The dotted line indicates the satellite tracks, while the heavy lines show where the satellites observed polar cap electron densities less than 10^4 cm^{-3}. The location of Qaanaaq is denoted by a circle which is filled for those times when Qaanaaq is underneath the polar hole. This sequence of snapshots clearly show that both the locaion and the spatial extent of the polar hole can vary significantly over several hours.

Figure 14 (Crowley et al., 1993) shows the UT variation of the polar hole measured for the minimum ion concentration from each DMSP satellite pass. The solid (open) circles denote the F8(F9) passes. The minimum values of approximately 10^3 cm^{-3} were observed near 10UT, corresponding to times when the hole was the largest. Based on the UT effect, the smallest values would be expected around 6UT. Hence, neither the extent nor the depth of the electron density depletion in the polar hole appear to follow the simple UT variation.

When Bz>0 the more complex cell structure of the convection pattern may enhance the polar hole. In the case of three or four cell patterns, there would exist regions of closed circulation within the polar cap. Without the transport of ionization from other locations into this region, these closed circulation regions have very little plasma production and therefore, lead to much deeper depletions than the two cell case by almost an order of magnitude at F-region heights. It is important to note that convection of ionization may help in enhancing or depleting a polar hole, however, this process could not produce the sharp boundaries observed which are correlated with the lack of electron and ion precipitation.

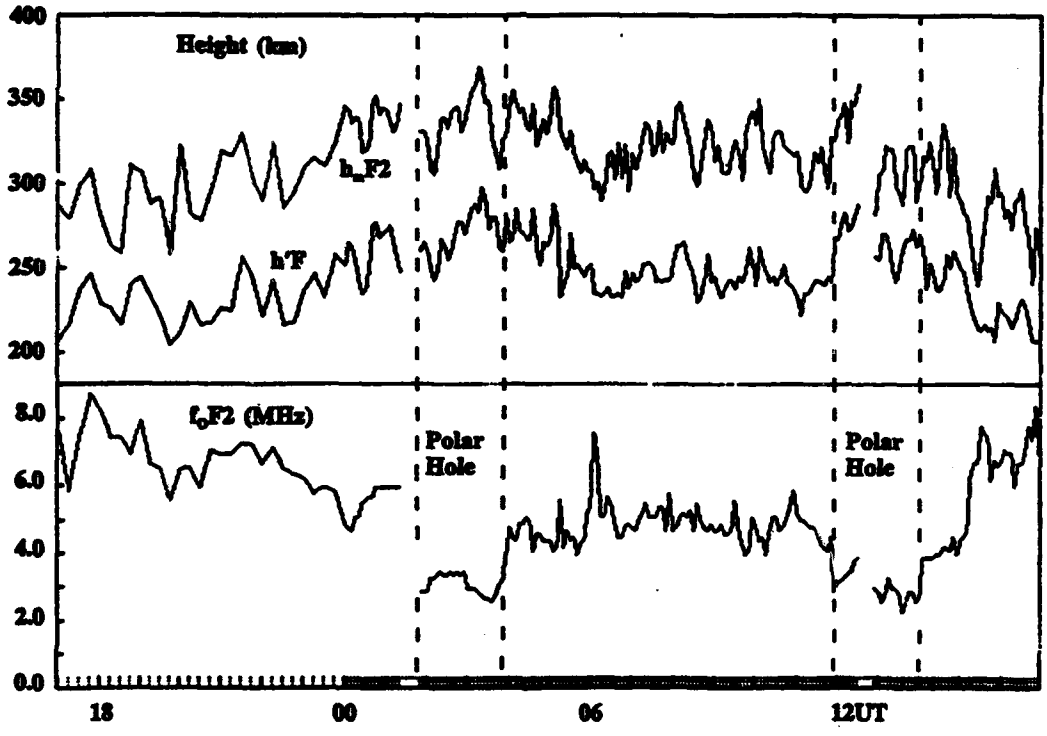

Figure 12. foF2, h'F and hmF2 variations measured at Qaanaaq for 5 & 6 January as the station crossed into the ionospheric polar hole (Crowley et al., 1993).

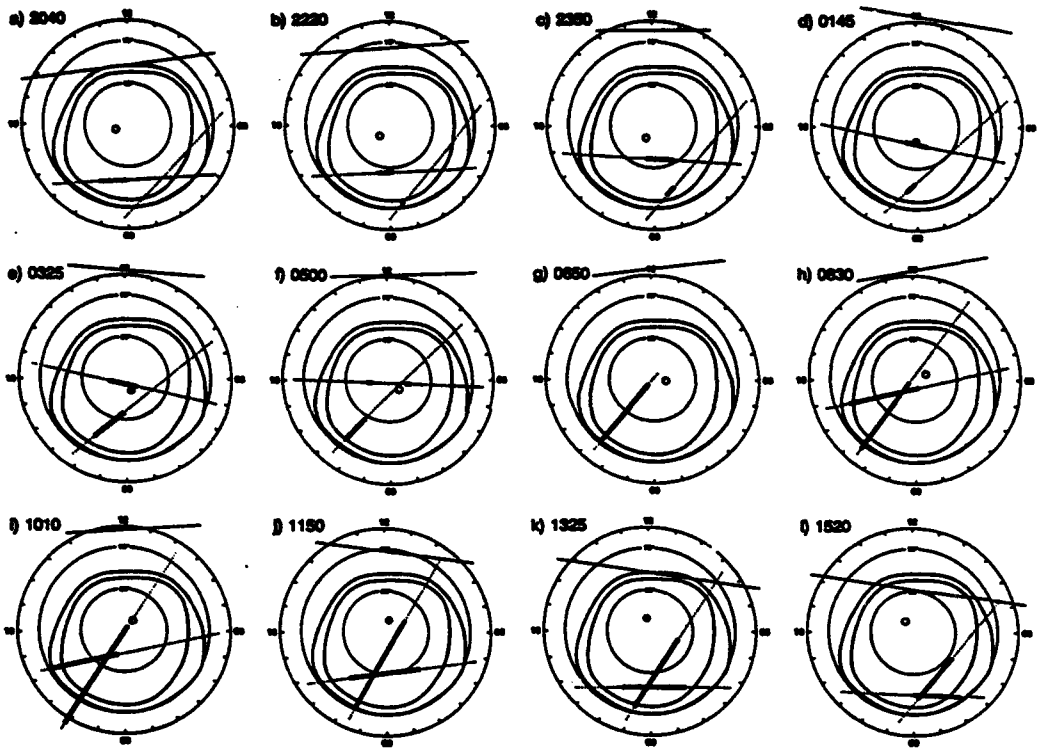

Figure 13. Development of the polar hole as a function of time for both DMSP F8 and F9 passes (Crowley et al., 1993).

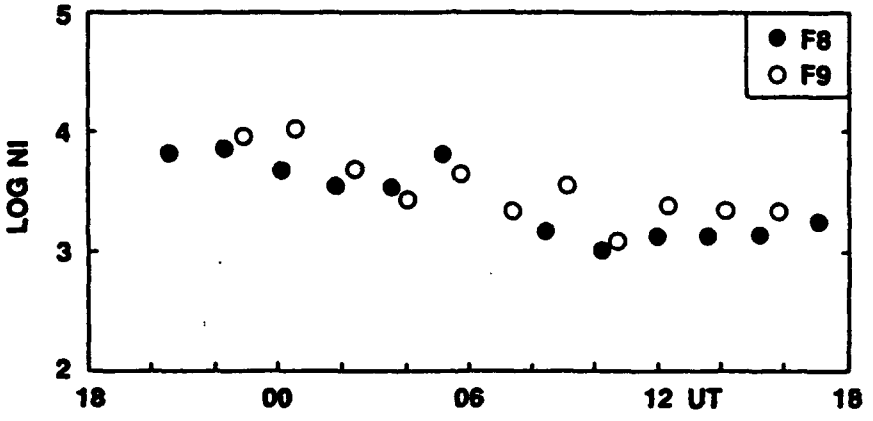

Figure 14. UT variation of the polar hole measured for the minimum ion concentration for each DMSP satellite pass.

4.3.2 The Mid-Latitude Trough

We have already seen an example of the mid-latitude trough which appeared as a depletion in the nightside electron density concentration at lower latitudes in Figure 11. In general, the mid-latitude trough which is observed in both hemispheres, is geo-magnetically orientated along a circumpolar region at an L-shell value of approximately 4, and was considered to be the boundary region between the mid-latitude and polar ionosphere.

Two of the most promising theories to explain the formation of the nocturnal trough are the so called "Stagnation Theory" [Knudsen, 1974; Spiro et. al., 1978] and the "enhanced recombination theory" [Banks et al., 1974; Schunk et. al., 1975]. Both of these theories stress the importance of plasma drift in trough formation. For example, rapid ion convection due to electric fields increases the ion temperature T_i by ion-neutral friction, which increases recombination rates and in turn lowers the electron density. In addition, the competing rotation of the earth and the westward plasma flow produce a stagnation region in which troughs are formed.

The study of the main trough involved establishing new methods to observe trough formations from large data sets. The trough detection ratio accomplishes this by specifying a number which indicates the presence of troughs. This detection ratio is defined as:

$$\rho_{hf} = \rho_{hmF2}/\rho_{foF2} \qquad (1)$$

where:

ρ_{hmF2} = (hmF2 observed) / (3-quiet day average of hmF2)

ρ_{foF2} = (foF2 observed) / (3-quiet day average of foF2)

Figure 15 (Scali and Reinisch, 1993) shows the diurnal variations of foF2 and hmF2, together with the horizontal and vertical velocity components measured by a Digisonde at Millstone Hill on 25 January 1990. The data are plotted as a function of Universal Time (UT), UT=LT+5h. The vertical component V_Z in the top panel varies from -25 to 25 m/s. The error bars represent one standard deviation determined from an ensemble of approximately 100 samples. The second panel, labeled V_h, displays the horizontal velocity components as vectors starting from the horizontal axis. The direction (in Corrected Geo-Magnetic) are given on the right by N(orth), S(outh), E(ast) and W(est) characters. The magnitude of the vectors specified by the 300 m/s scaling vector given on the left side of this figure, reaches values of 300m/s.

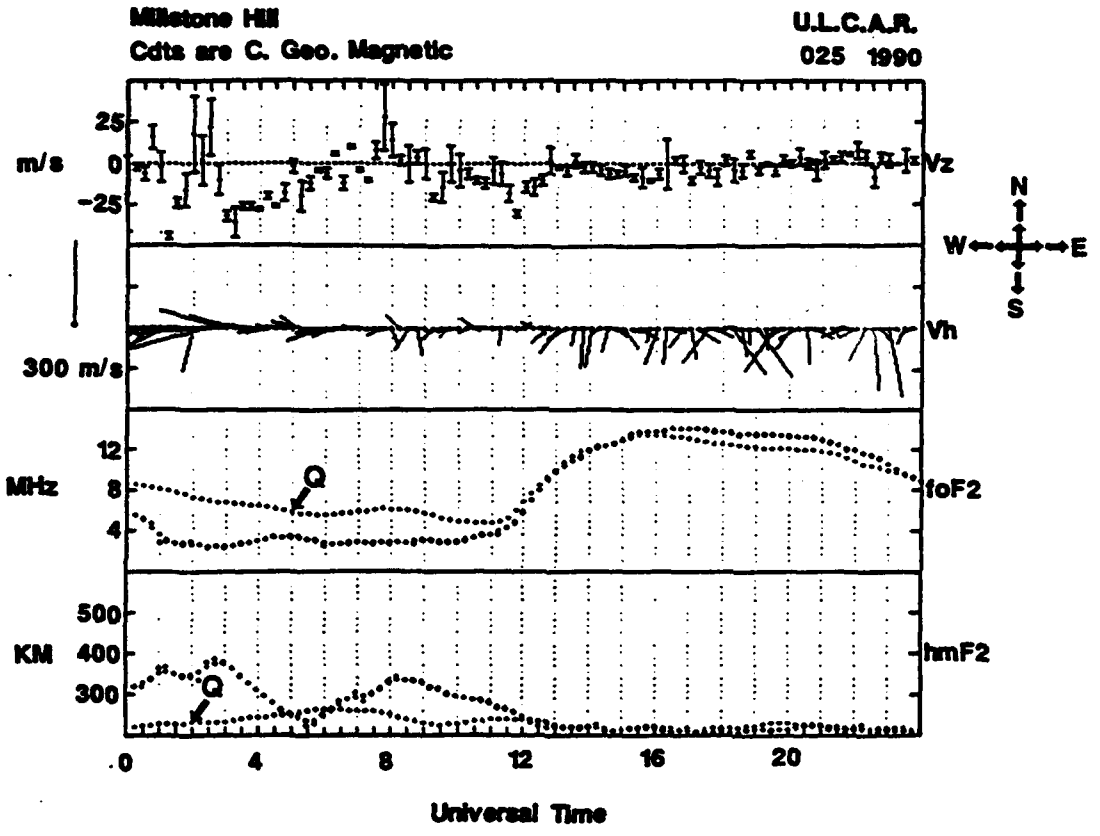

Figure 15. Diurnal variations of foF2, hmF2, the vertical velocity and the horizontal velocity components measured at Millstone Hill on 25 January 1990 (Scali and Reinisch, 1993).

The third and fourth panels compare the quiet day curves (labeled 'Q') and foF2, hmF2 current values. The 3-quiet day average curve for foF2 starts at approximately 8MHz at 00UT, while the January 25 curve begins at 6MHz. The two curves are similar between 12 and 16UT (07 to 11LT), but after 16UT the quiet day curve is usually lower until 24UT. A similar plot is shown for hmF2 on the fourth panel. The quiet day curve for hmF2 begins at 210km at 00UT and reaches a peak of 250km at 06UT, and after 12UT levels off to around 200-220km. The daily variation for January 25 starts at 300km at 00UT and reaches a peak value of 380km at 03UT, then falls to a value of 210km at 08UT. This figure illustrates the characteristic signature of a trough onset, i.e. a decrease to low values of foF2 and an increase to high values of hmF2. Hence, as a trough develops (hmF2/hmF2q)>1 and (foF2/foF2q)<1 which indicates that the trough detection ratio is large for significant troughs and unity when no troughs are present.

Figure 16 (Scali and Reinisch, 1993) shows the contour maps for ρ_{hf} plotted as a function of days and time for March 1990 at Millstone Hill, Argentia and Goose Bay. Since we consider only well developed troughs in this study, the plotted ρ_{hf} contours begin at ratio values of 1.6 or greater. It is clear from this figure that for the month of March 1990 at least two distinct periods of trough formation were observed at all stations. These periods are for the days 71 to 73, and 80 to 89. The vertical bars below each graph indicate the availability of data over a 24 hour period. If no vertical bar exists, no data was collected for that day. As an example, for days 82 to 84 at Argentia, no data was recorded. This explains the lack of trough detection ratios during this time.

In Figure 16, troughs are generally formed prior to 00UT (before sunset) at Goose Bay, while at the lower latitude stations of Argentia and Millstone hill, troughs are observed after sunset (00UT). The formation of troughs at these times correlate with well organized westward drift. Figure 17 (Scali and Reinisch, 1993) shows the horizontal velocity and trough ratio mapped on a polar plot for day 90047 at Millstone Hill. On this day, the main trough was first detected at approximately 19 CGLT, identified by large ρ_{hf} values. The velocity dramatically increases in magnitude during this time period, pointing in the SW direction with a strong component opposite the rotation velocity vector. The drift reaches a maximum value of approx. 550m/s. The earth's angular rotational velocity for this station at F-

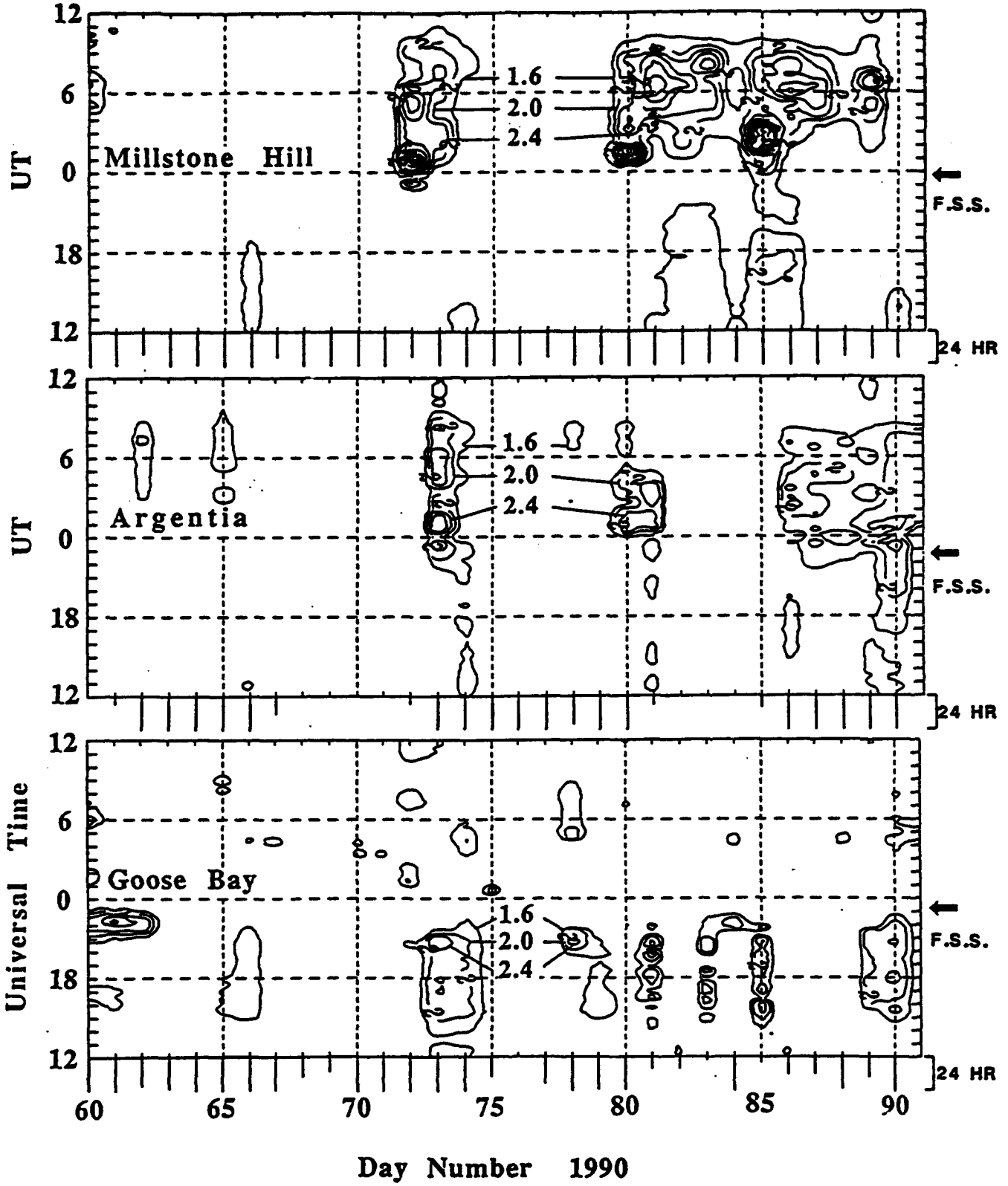

Figure 16. Trough detection contour maps for the month of March 1990 calculated from measurements made at Millstone Hill, Argentia and Goose Bay (Scali and Reinisch, 1993).

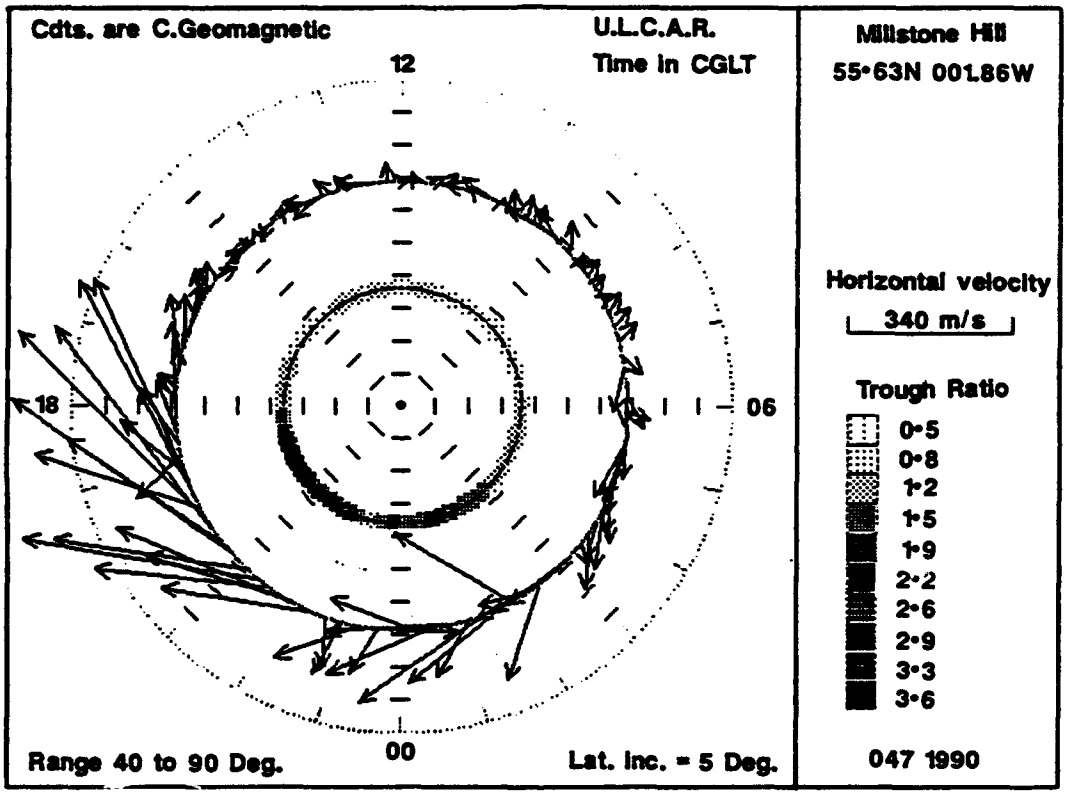

Figure 17. Polar plot of the horizontal velocity and trough detection ratio measured at Millstone Hill on 16 February 1990. The development of a trough is correlated with increased westward velocity drifts opposing the co-rotation of the earth.

region heights (300km) is given as 357m/s. A second maximum of ρ_{hf} at 01CGLT is also associated with large drift vectors of about 430m/s. Thereafter, the horizontal speed decreases to 115m/s. The westward drifts opposing the co-rotation of the earth slow the plasma movement. The ionization confined to this region begins to decay and even under normal recombination processes, the electron density falls to very low values. These results illustrate that the deep troughs form and develop quickly in regions where the plasma flow has been stagnated as is expected from the Stagnation Theory.

The conditions necessary to establish a stagnation region are always present, i.e. westward drifts are observed consistently at night at Millstone Hill. All that is required is that induced electric fields increase the horizontal velocity magnitudes to values comparable with the co-rotation of the earth. Figure 18 shows the horizontal velocity contours plotted for each day in March 1990. In the second plot for the azimuthal direction of the horizontal velocity component, only contours for 180 to 360 degrees are plotted and angles between 260 and 280 degrees are shaded in black. Throughout the entire month, horizontal velocities predominantly point eastward from 10 to 20UT (Daytime) and westward at night. In comparison with Figure 16, deep troughs are produced when the magnitude of V_h is large. The formation of the mid-latitude trough is related to the increased velocities due to induced electric fields.

Further analysis of the detection of the mid-latitude trough was conducted by using oblique propagation sounding from Goose Bay and Argentia. Figure 19 shows the trough detection ratio for Millstone Hill, Argentia and Goose Bay, calculated for data recorded during the month of August 1990. Two distinct periods of trough formation were detected. On day 90228 a trough formed at Goose Bay at approximately 01UT. At approximately 05UT a trough was observed at Argentia, while around 07UT Millstone Hill detected a trough. The onset of the troughs observed at each station on day 90228 illustrate the progression of movement of the trough to lower latitude as a function of time.

On day 90233 at 19UT a trough was detected at Goose Bay. On day 90234 at 00UT a trough began forming at Argentia and later at 01UT, Millstone Hill detected the

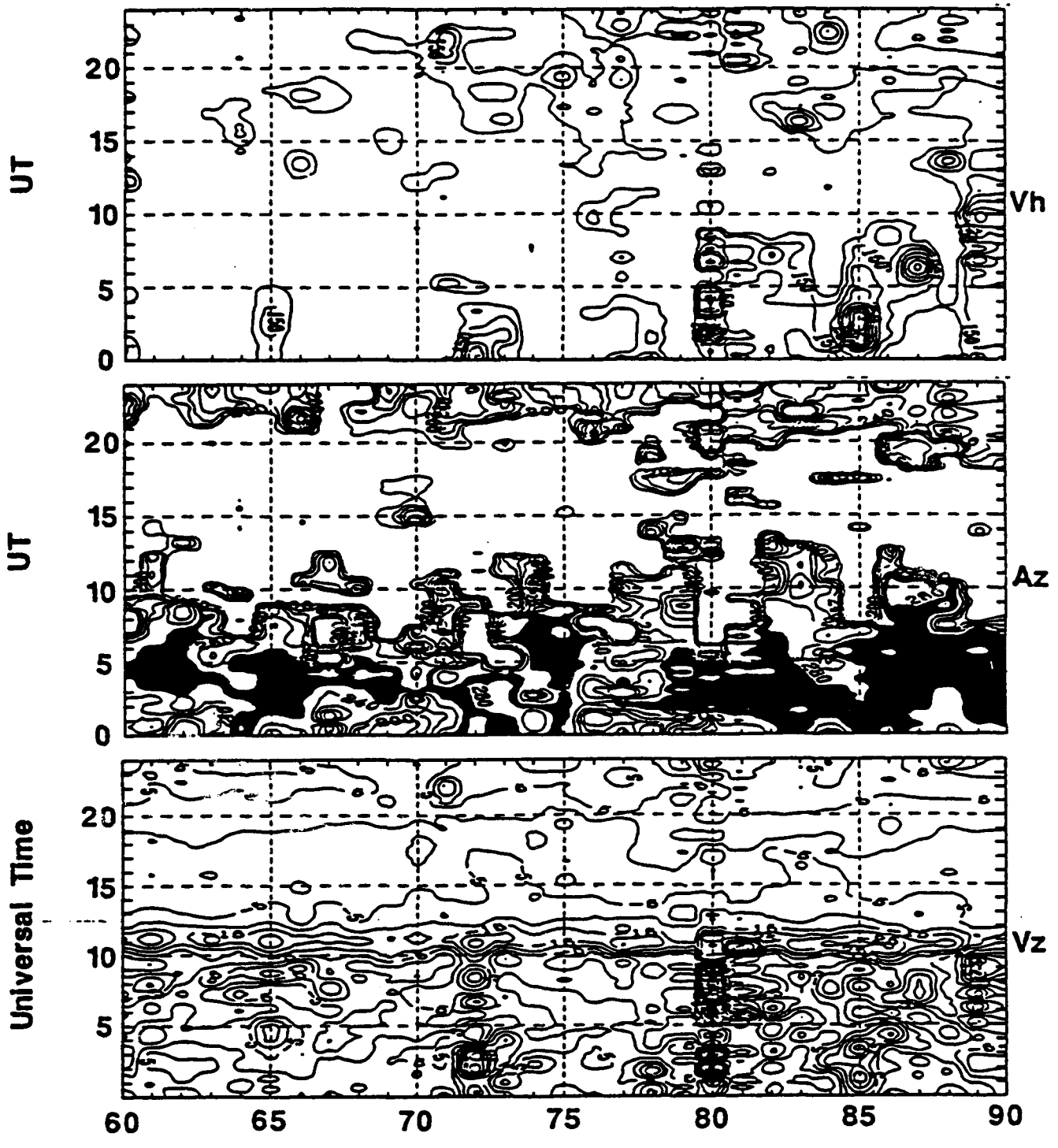

Figure 18. Horizontal and vertical velocity contours for data recorded at Millstone Hill during March 1990. In second graph for Az only, contours for angles 180 to 360 are shown. The shaded region corresponds to time when the horizontal drift velocity vector angle is between 260 and 280 degrees..

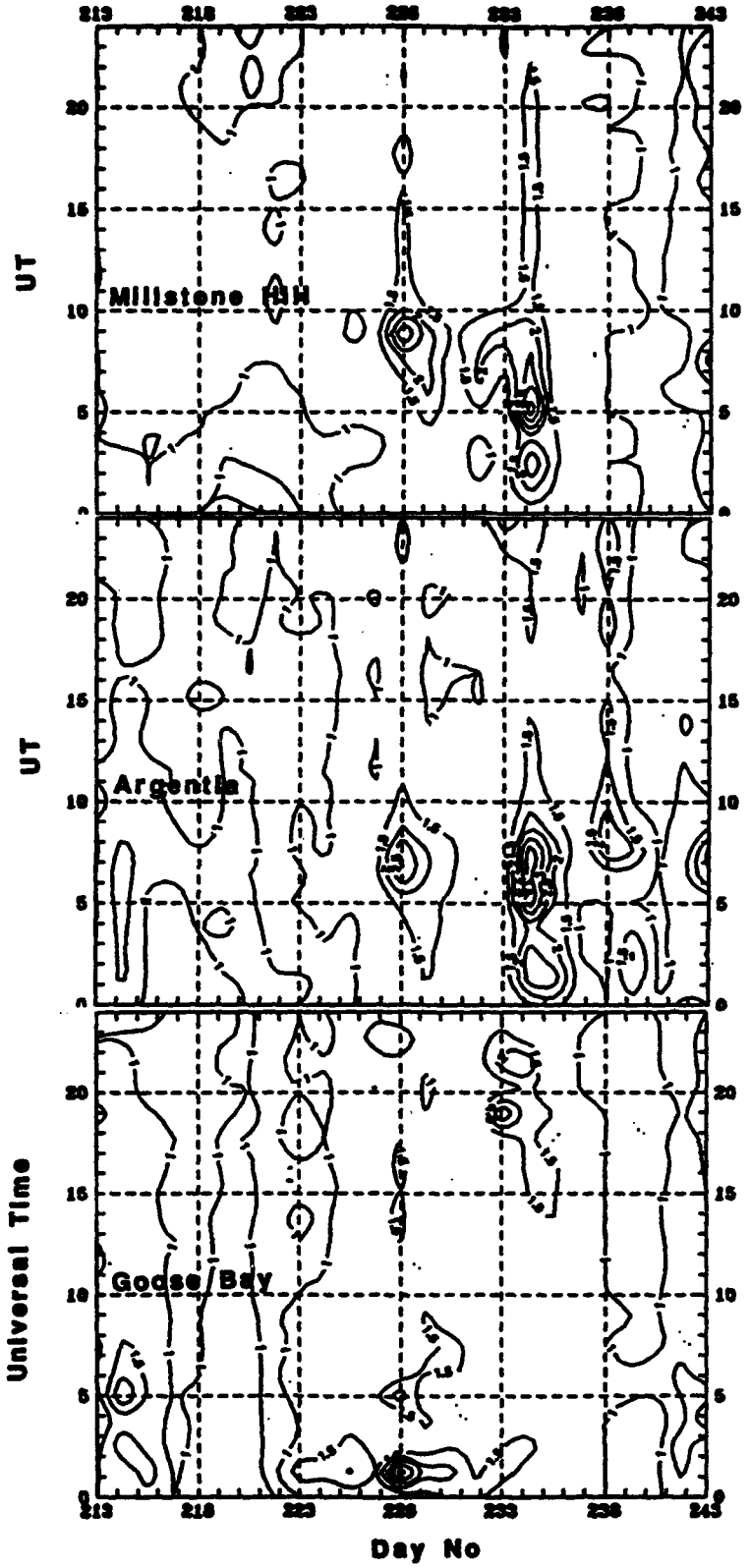

Figure 19. Trough detection ratio contours measured at Millstone Hill, Argentia and Goose Bay during August 1990. Contour intervals in each plot are 0.5 and only ratios ≥ 1.0 are displayed.

formation of a trough. The effect of this trough on oblique propagation between Goose Bay and Argentia is observed in Figure 20. This figure displays a sequence of oblique ionograms recorded at Goose Bay. The oblique ionograms scan from 9 to 19 MHz. The traces are easily identifiable for both polarizations from 2010 to 2255UT, even though a trough has formed over Goose Bay at this time. As the mid-latitude trough approaches Argentia, the oblique ionograms begin to be severely effected. At 2325UT, multiple reflection paths produce multiple oblique traces. Shortly after this time, as the trough begins to develop over Argentia, the MUF is reduced below 9MHz and is out of the scanning field of view. In the future the actual shape of the oblique traces will be further investigated in order to determine the precise propagation paths of the radio waves as they transverse the mid-latitude trough.

4.4 ISR/DGS Drift Comparisons

The Digisonde at Sondrestrom represents an important link in the high-latitude network due to its unique geophysical location in the dayside cusp region and also because of the co-location of an Incoherent Scatter Radar (ISR) facility. In this section, a two day comparison of the horizontal drift vectors measured by both instruments is presented.

In Figure 21 the horizontal drift velocity magnitude and azimuthal angle of arrival are plotted for day 91339. The continuous line represents velocities calculated by the ISR while the dashed line represents velocities calculated by the Digisonde. On the whole, the two instruments tend to measure the same velocities, especially in the cusp region where the horizontal velocities quickly change from westward to eastward as the station moves from the dawn to the dusk convection cells.

Comparing another data set recorded on 91342 (Figure 22), again the velocities measured by both instruments are in close agreement. The azimuthal angle of arrival for the horizontal drift for this data set is in extremely good agreement. Further statistical comparisons need to be done with this data, but from the data sample currently analyzed both instruments are measuring the same drift velocities. It is difficult in light of these results to explain the observed systematic errors

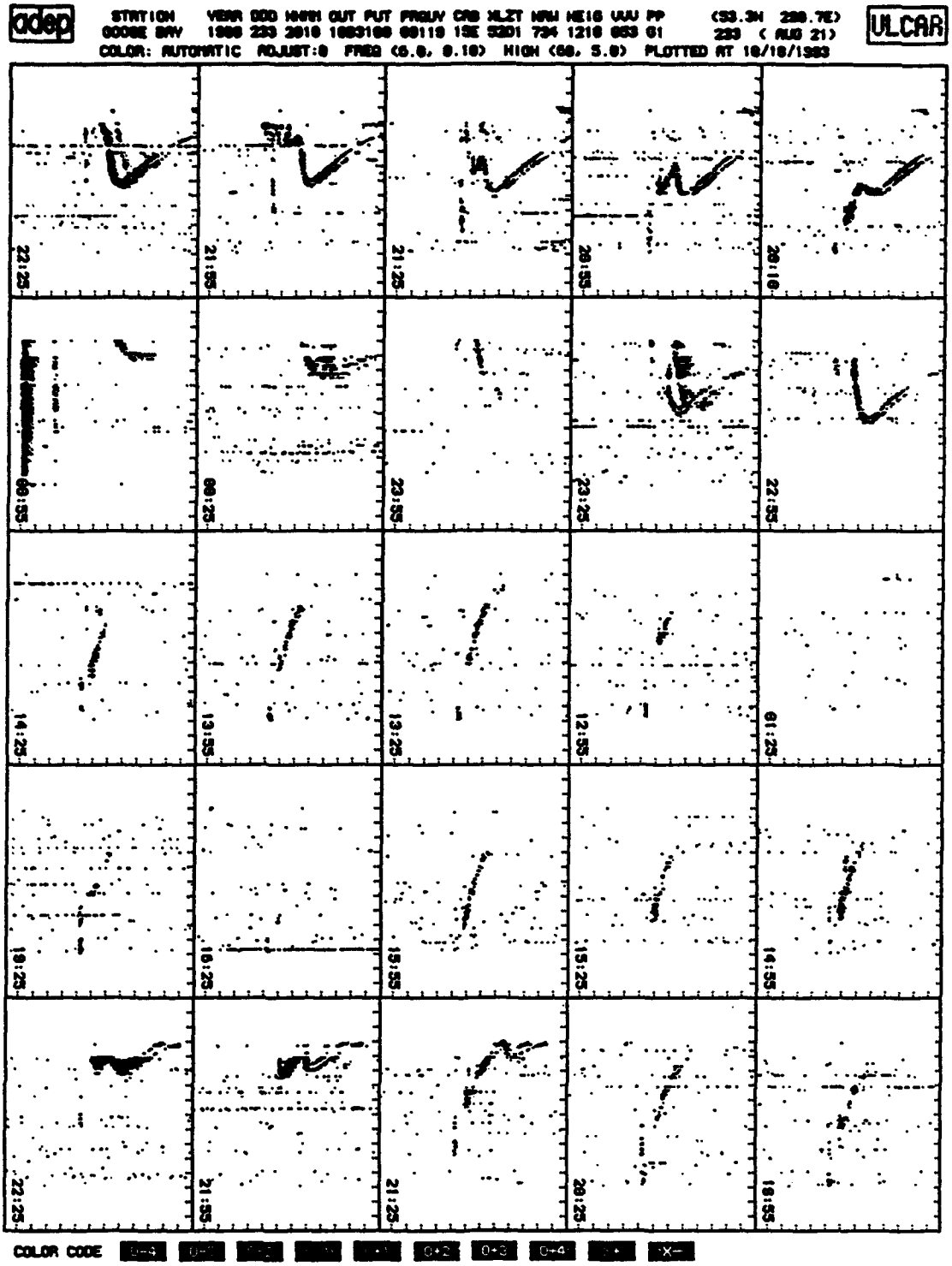

Figure 20. Sequence of oblique ionograms measured at Goose Bay for propagation path from Argentia to Goose Bay. On this day a trough developed and moved over both stations.

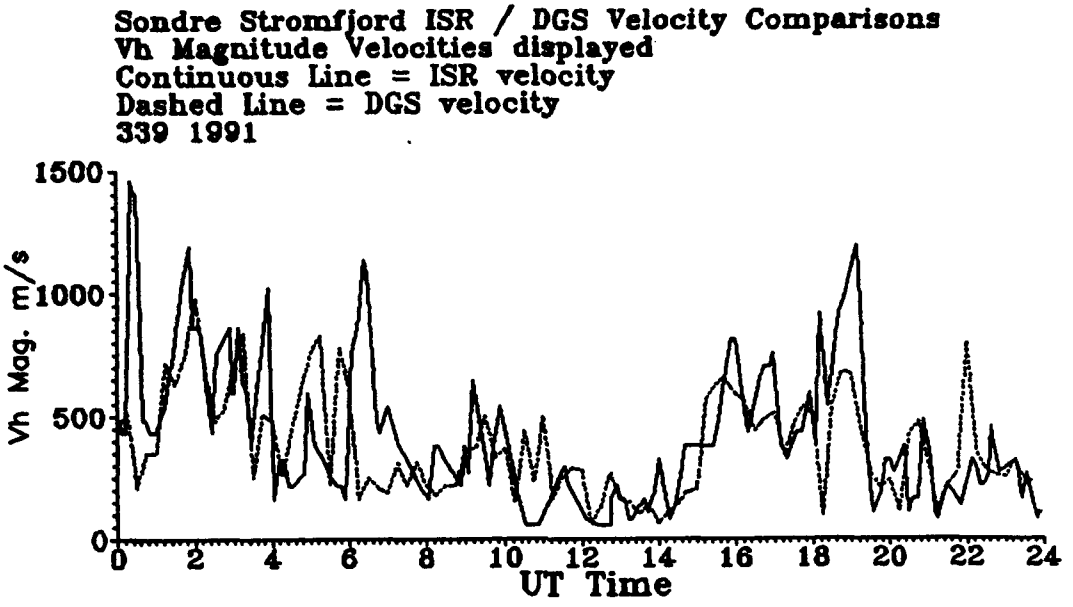

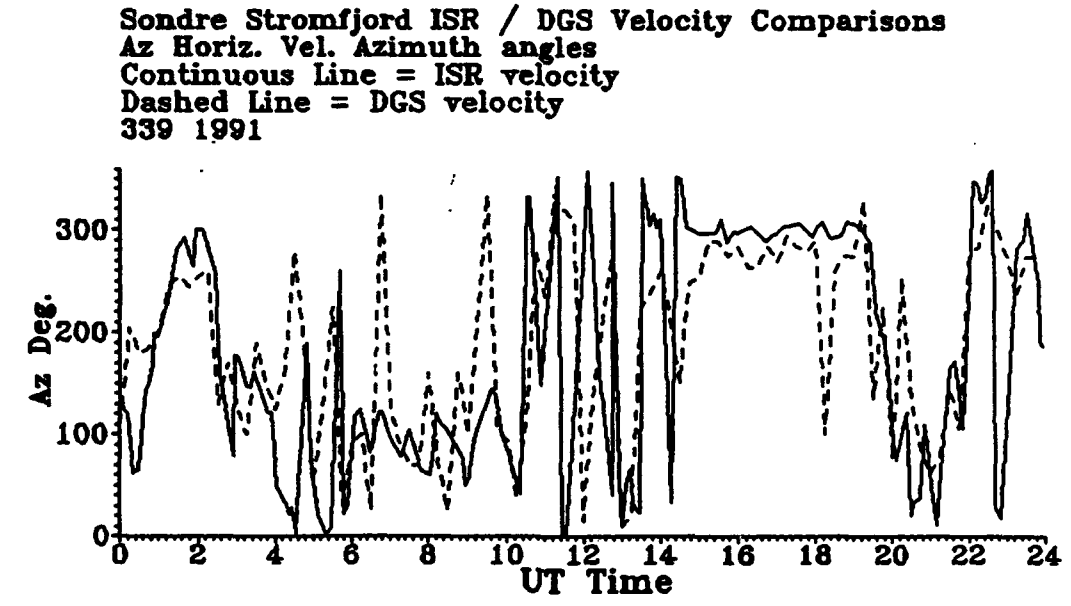

Figure 21. ISR and Digisonde horizontal drift velocity, magnitudes and azimuth angle of arrival for day 39, 1991.

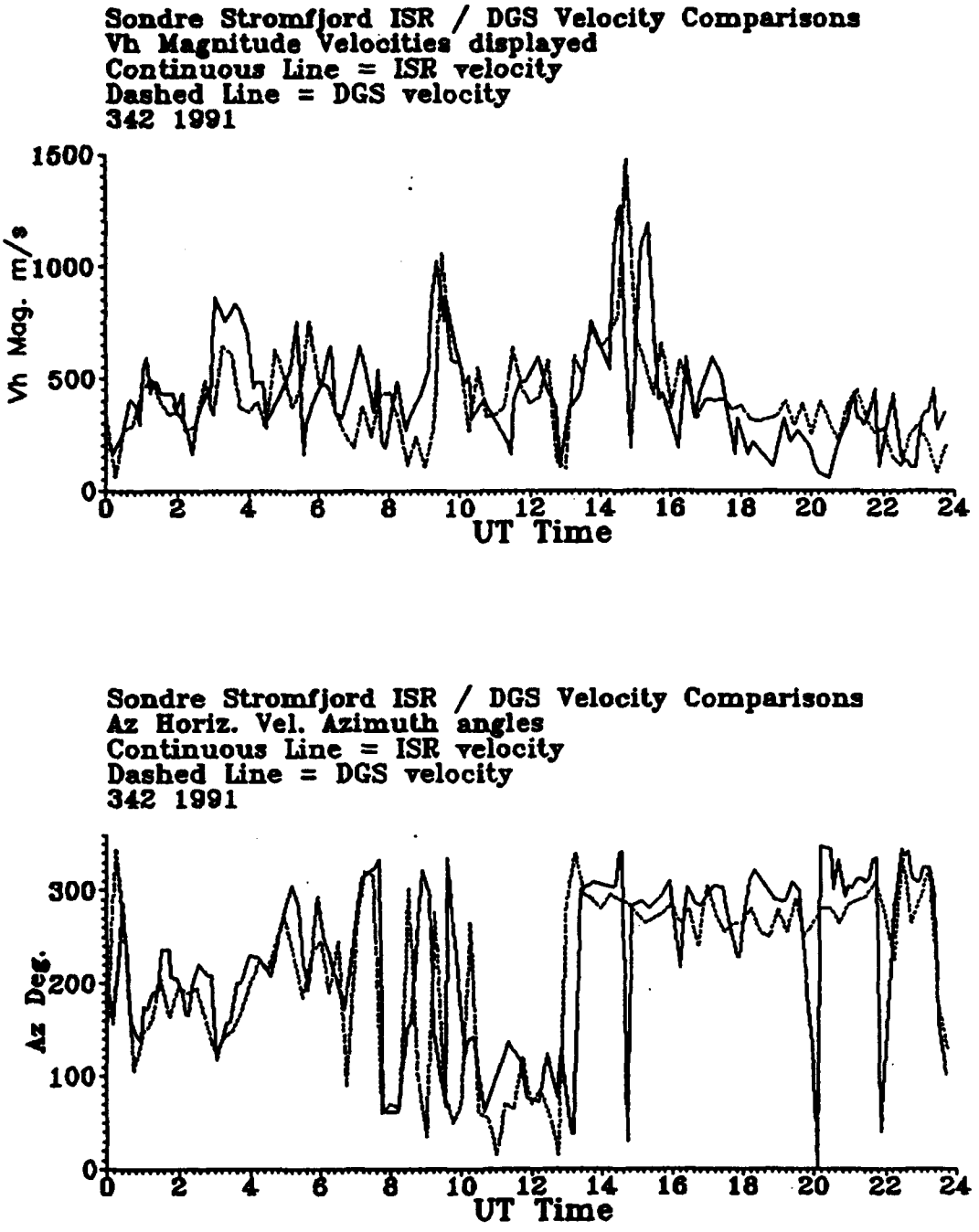

Figure 22. ISR and Digisonde horizontal drift velocity, magnitude and azimuth angle of arrival for day 342, 1991.

observed in the comparison of Qaanaaq and DMSP velocities made for drift data collected in 1987. The configuration upgrade at Sondrestrom operates faster drift modes and an improved drift velocity calculation scheme. Considering the ISR/DGS velocities compare well, it is recommended that Qaanaaq be similarly upgraded and a new comparison be carried out.

4.5 Sondrestrom ODDA results

During June 1992 the Digisonde system at Sondrestrom was upgraded to run the new ARTIST3/ODDA system. This system not only incorporated major improvements for the I/O communications, data recording, ionogram scaling and profile inversion, but for the first time drift velocities were calculated and displayed in real time. The Onsite Digisonde Drift Analysis (ODDA) package manipulates the drift data in two ways. ODDA uses the drift data to assess the performance of the Digisonde system. The quality control package attempts to verify that no major problems exist and relate the system status to the operator. (Scali Scientific Report #13, 1993). This allows problems to be quickly identified and corrected rather than continuing unnoticed for extended periods of time. The drift data is then used to calculate skymaps and velocities.

The velocities are displayed onsite and stored along with the Skymaps and raw drift files to cartridge tape. This removes a great deal of post processing previously required to obtain velocity data from raw drift data recorded to tapes some time ago. Since June 1992 the Digisonde system at Sondrestrom has been recording ionograms, ARTIST results, raw drift, Skymaps and velocities. To assess if ODDA was operating properly, data recorded at Sondrestrom was later processed at ULCAR with inhouse programs.

Figures 23 and 24 shows two Skymaps. Figure 23 displays the skymap data calculated at the station immediately after the drift data was recorded. The Skymap data files stored on cartridge tape were extracted without the need for post processing. The reflection point locations are displayed with their associated radial velocities. A radial velocity pointing inward (Blue coded) specifies positive Doppler shift, while a radial velocity pointing outward (coded red) specifies a negative Doppler shift. In

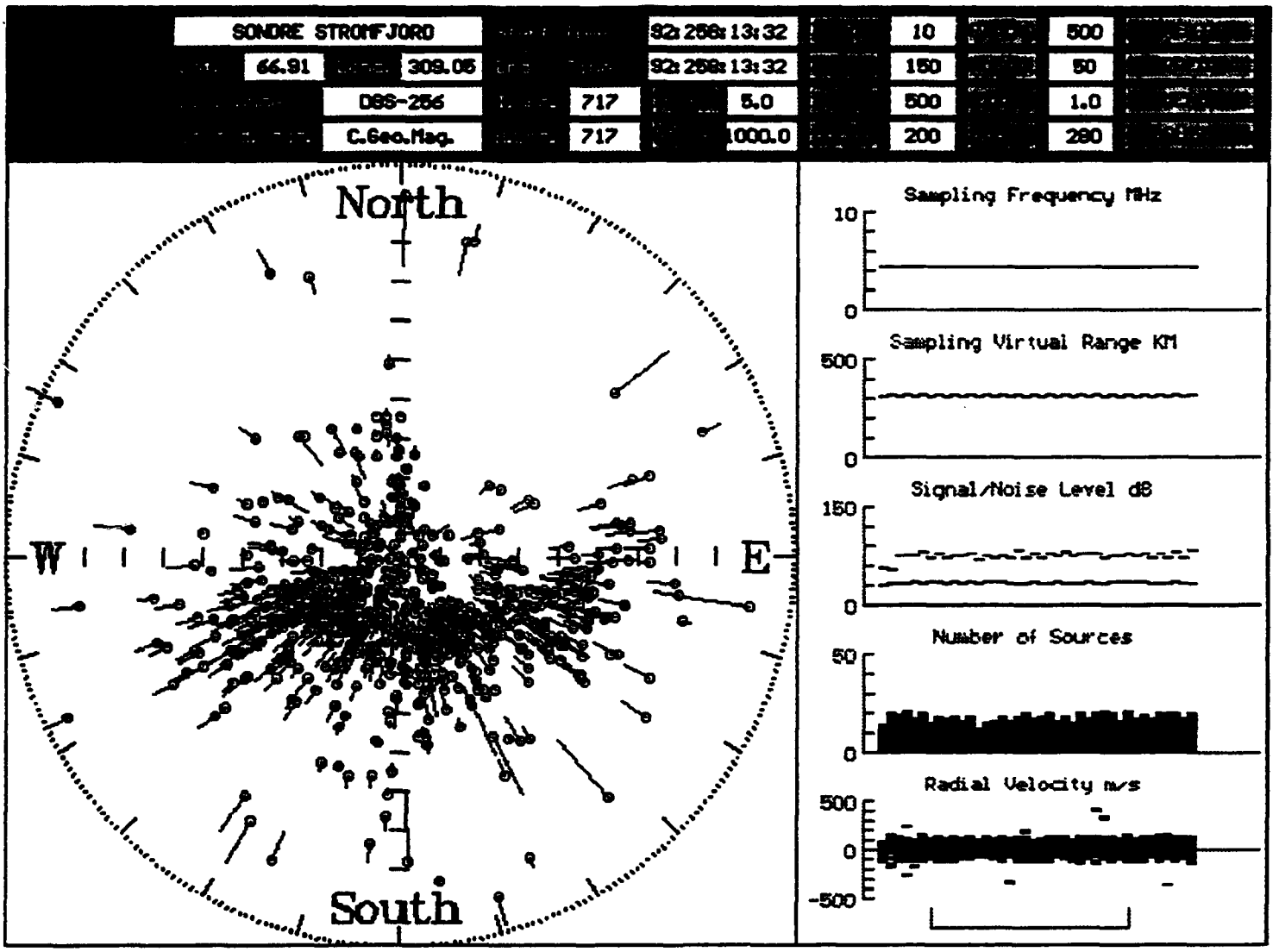

Figure 23. Skymap of ODDA data calculated at Sondrestrom in real time and extracted from cartridge tape. Skymap calculated on day 258, 1992.

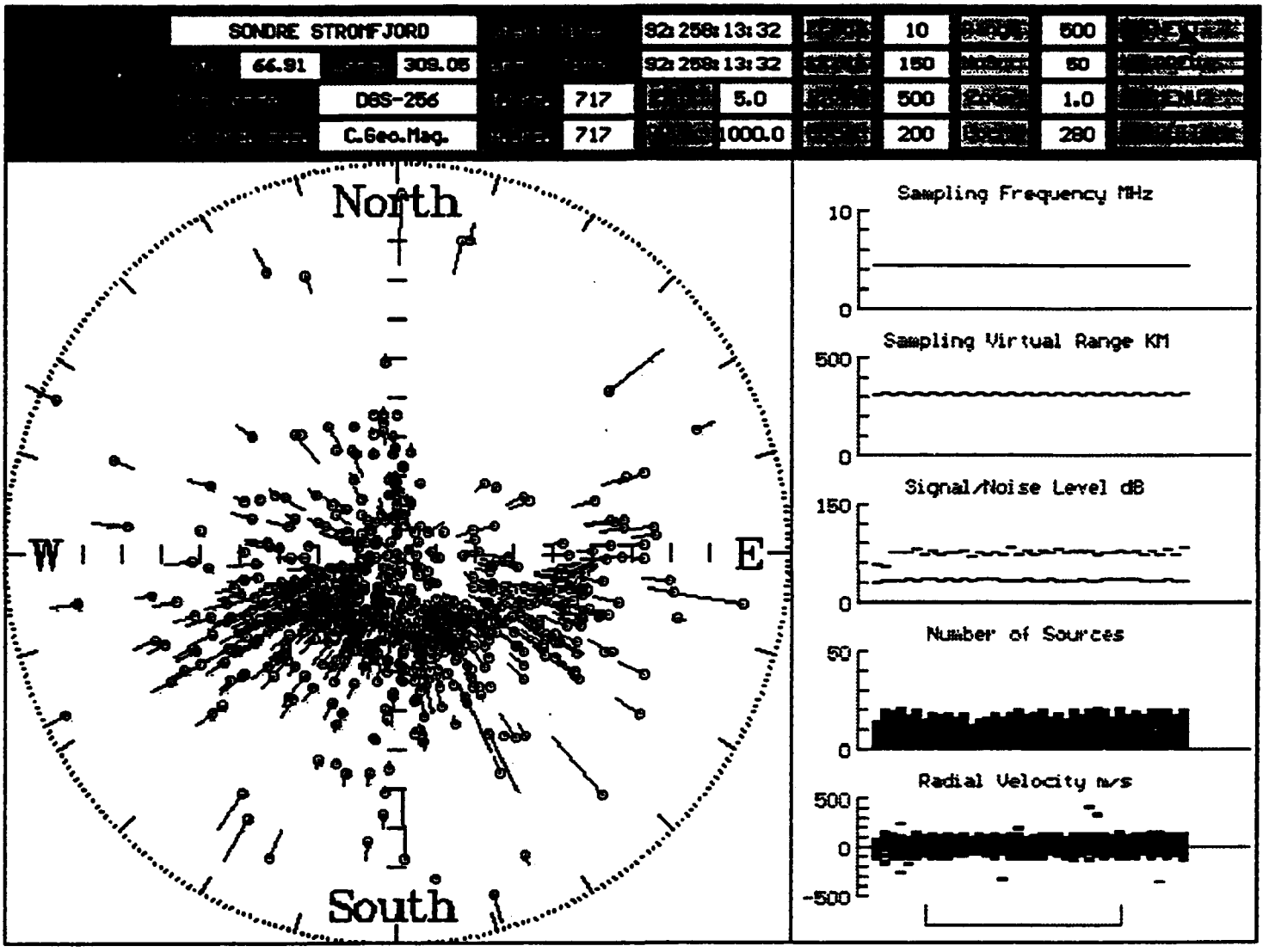

Figure 24. Skymap calculated from in-house program (DDA) using raw drift data from cartridge for data recorded on day 258, 1992. Post-processing of data.

this plot 40 height spectra are gathered and 717 sources are displayed. The linear graphs on the right display specific information for each height spectra such as sampling frequency, sampling height, signal and noise levels, number of sources detected in each height spectra and the radial velocity on each source.

ULCAR received the tape for analysis a few weeks after the measurements were made. Using the drift data recorded to cartridge and the inhouse Digisonde Drift Analysis package (DDA), a skymap file was generated. For the same time period as given in Figure 23 the post processed skymap data is plotted in Figure 24. The two plots are identical. Extensive manipulation of the skymap data indicated that ODDA was correctly calculating source positions at the field site.

Next the velocity data calculated by ODDA at Sondrestrom was retrieved from the cartridge tape. The results are shown in Figure 25. From previous research conducted in cusp studies at Sondrestrom the characteristics of what to expect at this station are well known. In Figure 25 the vertical velocity, horizontal velocity magnitude and the azimuthal angle of arrival of the horizontal velocity vector are plotted for results recorded on days 92259-92261. Superimposed on the azimuthal angle of arrival plot is the azimuth variation expected for a simple two cell convection pattern. The expected and actual horizontal velocity azimuthal angles agree very well, and it is easy from this data set to observe the cusp region around 12CGLT each day.

Horizontal magnitudes are observed to be on average 750m/s. The vertical velocities tend to show a diurnal dependence, with negative velocities observed near the cusp region and positive velocities in the dawn sector. Most of the skymap and velocity data calculated from ODDA and extracted from the cartridge tape are of good quality, and the convection patterns are clearly defined. From the performance of ARTIST3/ODDA system at this station, it is highly recommended that other stations be similarly upgraded and use is made of the real time electron density profiles and velocities.

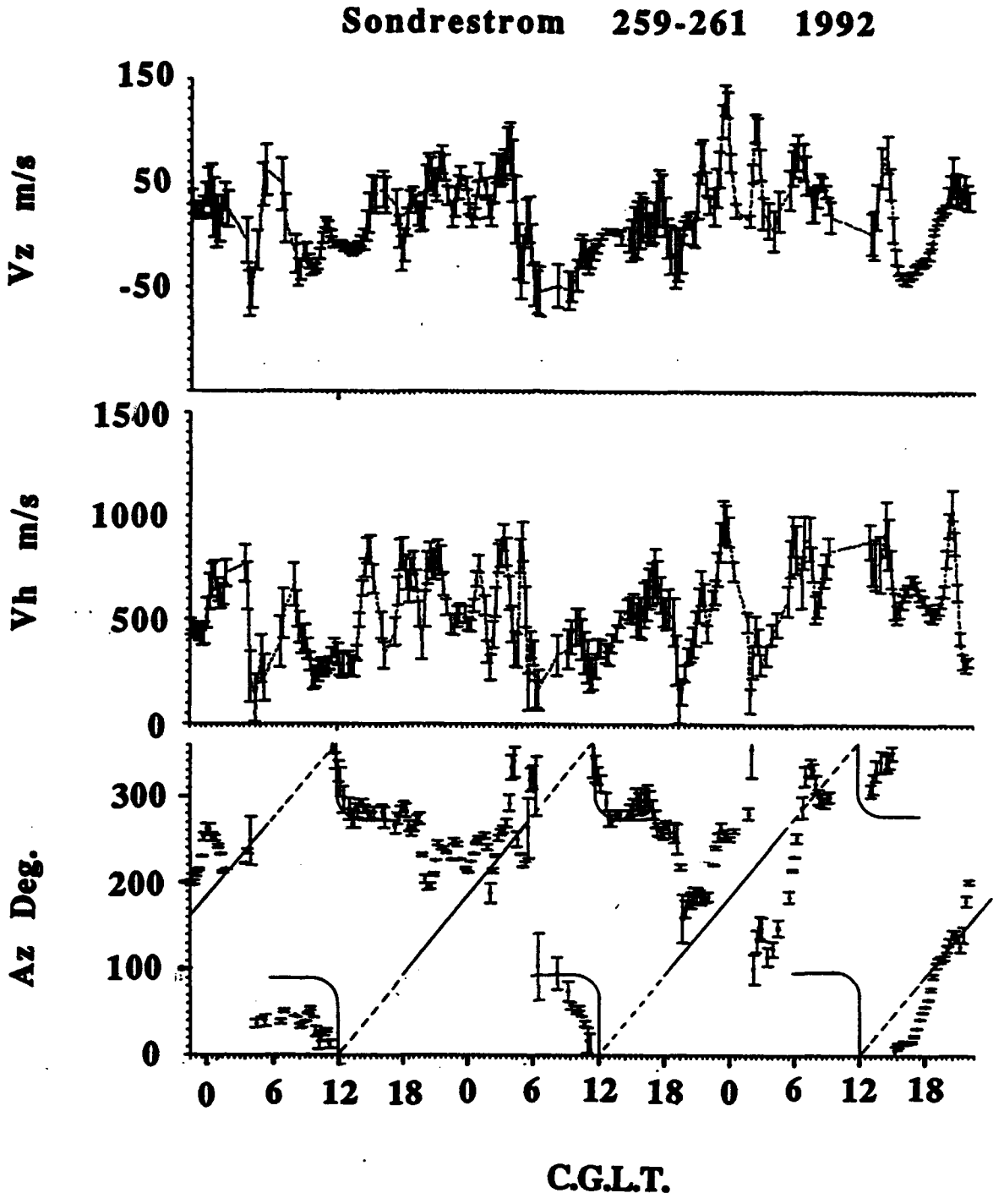

Figure 25. ODDA real time calculated data for the vertical velocity "Vz", the horizontal velocity magnitude "Vh", and the azimuthal angle of arrival "Az". Data collected directly from cartridge with no post-processing.

5. SUMMARY AND CONCLUSIONS

During the period from October 1989 to October 1993, a substantial data set of ionospheric and plasma drift velocities were collected by various instruments. The analysis of these data sets improved the understanding of the physics of the F-region dynamics. The goals specified originally for this project were all met and the main achievements in this study can be listed as:

1. The Digisonde at Sondrestrom was upgraded to run new and faster drift modes, and the ARTIST3/ODDA system successfully installed. This made Sondrestrom the first station to supply electron density profiles and drift velocities in real time. The ODDA package incorporates a Quality Control scheme that quickly identifies when major problems occur and relates the system status to the operator. The calculation of the velocities in real time removes the need for post processing making this data immediately available. The calculated velocities obtained from the ODDA system operating at Sondrestrom are of high quality, and major convection structures such as the daytime cusp and Harang discontinuity regions are consistently identified. This real time ability may be extended to other stations to produce a real time snapshot of the convection pattern over the polar cap.

2. Comparisons of the ISR and Digisonde data sets indicate that both instruments are measuring the same drift velocities. The horizontal velocity magnitudes are approximately of the same order and the horizontal azimuthal angle of arrival are in good agreement, especially at those times when the station is crossing into the dayside cusp region.

3. The study of patch formation outlines convection patterns that transport patches of enhanced electron density concentrations into the polar regions. The Digisonde ionograms help identify the patch structure as it moves over the station, which is used to track the movements of these patches. Velocities measured at Sondrestrom show that the ionization movement in the cusp region may behave much like a vortex, pulling sub-cusp plasma into the polar anti-sunward flow.

4. Polar convection monitoring using a network of Digisonde stations is possible. The statistical analysis of the Digisonde data at Qaanaaq has already improved the understanding of the F-region convection pattern during different IMF B_Z and B_Y conditions. The results show that the sign of the IMF Bz component controls the coarse structure of the convection pattern (i.e. either two or more cells). The B_Y component controls which field lines best contribute to the polar convection pattern, and so variations in B_Y are outlined by the distortion of the two or four cell systems. The relationship between the convection in the Polar Cap and the orientation of the IMF B_Z and B_Y components is so evident that, even for a single station using the Digisonde drifts, the sign of the IMF B_Z and B_Y components can be determined to better than 60%. Folding drift data from other stations (such as Sondrestrom) will improve the accuracy in the determination of the IMF orientation, as well as clearly defining the convection pattern established.

5. The study of the Ionospheric Polar Hole indicated that this phenomena is confined to regions where a lack of electron and ion precipitation occurs, which is consistent to a closed field line environment. Analysis of the convection patterns associated with the Polar Hole show the movement of ionization in and out of this region may contribute to enhancing or depleting the electron density levels. But convection alone cannot account for the sharp boundaries observed for the Polar Hole. Measurements of hmF2 and foF2 made at Qaanaaq support the closed field line theory, which produces the greatest amount of electron depletion at the boundaries as compared to the middle of the Polar hole region.

6. Unlike the Ionospheric Polar Hole, the Mid-Latitude trough develops quickly in regions where the plasma flow has been stagnated due to increased westward horizontal flow of the plasma opposing the co-rotation of the earth. The conditions necessary for trough formation is always present, i.e. westward drifts are consistently measured at night in sub-auroral regions. All that is required is an induced electric field increase the horizontal velocity magnitude to values comparable with the co-rotation of the earth.

The completed project has shown the necessity of combining as many instruments as possible in order to develop a complete picture of the Polar convection pattern, and associated phenomena. However, without the consistency of a continuous data base as offered by Digital ionosondes, much of the statistical analysis of the

convection and ionospheric structures could not have been possible. The results have shown that it is now possible to go to a real time data acquisition scheme, in which a network of Digisonde stations supplemented occasionally with DMSP and/or ISR measurements, can provide a snapshot of the convection pattern and structures at high latitudes.

6. LIST OF PUBLICATIONS / CONFERENCE PAPERS

6.1 Conference Papers

Buchau J., G Crowley and B.W. Reinisch, "First Results from the Digisonde at Sondrestrom," URSI, Boulder, Colorado, January 1990.

Cannon P.S., B.W. Reinisch, J. Buchau, G. Crowley and R. Lepping, "IMF Controlled Variations in the Convection Flow Direction Near the Corrected Geomagnetic Pole," URSI, Boulder, Colorado, January 1990.

Scali J.L. and B.W. Reinisch, "Spread-F Structure Observed at Mid-Latitude Stations Using a Digisonde 256," CEDAR Workshop, 12-16 June 1990.

Crowley G., J. Buchau, B.W. Reinisch and P. Hoeg, "Cusp Signatures from the Digisonde," Geospace Environment Modeling Conference (GEM), October 1990.

Scali J.L. and B.W. Reinisch, "The Characteristics of the Mid-Latitude Trough as Observed by Digisonde 256 Observations," URSI, Boulder, Colorado, London, Ontario, Canada, 1991.

Crowley G., B.W. Reinisch, P.S. Cannon and J. Buchau, "Digisonde Polar Convection Studies for Bz North at Qaanaaq, Greenland," November 1991 - January 1992.

Scali J.L. and B.W. Reinisch, "Measurement of Drift Velocities at the Dusk Sector Mid-Latitude Trough," CEDAR Workshop, 12-16 January 1992.

Crowley G., C.G. Dozois and B.W. Reinisch, "Measurements of Polar Cap Convection for Bz North," CEDAR Workshop, 12-16 January 1992.

6.2 Scientific Reports

Scali J.L. and B.W. Reinisch, "Measurements of F-region Drift Velocities at the Dusk Sector Mid-Latitude Trough," Scientific Report No. 1, PL-TR-92-2094, ADA257766, March 1992.

Scali J.L., "The Mid-latitude Trough, A Review," Scientific Report No. 2, PL-TR-92-2100, ADA258606, April 1992.

Scali J.L., "A Quality Control Package for the Digisonde Drift Analysis (DDA)," Scientific Report No. 3, PL-TR-93-2220, October 1993.

6.3 Publications

Buchau, J. and B.W. Reinisch, "Electron Density Structures in the Polar Region," Adv. Space Res., Vol. 11, No. 10, pp. 29-37, 1991.

Cannon P.S., B.W. Reinisch, J. Buchau and T. Bullett, "Response of the Polar Cap F-Region Convection Direction to Changes in the Interplanetary Magnetic Field: Digisonde Measurements in Northern Greenland," J. Geophys. Res. Vol. 96(A2), 1239-1250, 1991.

Crowley G., P.S. Cannon, C.G. Dozois, J. Buchau and B.W. Reinisch, "Polar Cap Convection for Bz Northward," Geophys. Res. Lett., Vol. 19, pp 657-660, 1992.

Cannon, P.S., G. Crowley, B.W. Reinisch and J. Buchau, "Digisonde Measurements of Polar Cap Convection for Northward Interplanetary Magnetic Field," J. Geophys. Res. Vol. 97(A11) 16877-16885, 1992.

Crowley, G., H.C. Carlson, S. Basu, W.F. Denig, J. Buchau and B.W. Reinisch, "The Dynamic Ionospheric Polar Hole," Radio Science, Vol. 28, No. 3, pp 401-413, 1993.

Scali J.L. and B.W. Reinisch, "F-Region Drift Velocities in the Dusk Sector Mid-Latitude Trough," Submitted to J.A.T.P., 1993.

7.0 REFERENCES

Anderson, D.N., J. Buchau and R.A. Heelis, "Origin of Density Enhancements in the Winter Polar Cap Ionosphere," Radio Science, Vol. 23, pp. 513, 1988.

Banks, P.M., R.W. Schunk and W.J. Raitt, "NO^+ and O^+ in the High Latitude F-Region," Geophys. Res. Lett., Vol. 1, pp. 239-242, 1974.

Heelis, R.A., P.H. Reiff, J.D. Winningham and W.B. Hanson, "Ionospheric Convection Signatures Observed by DE During Northward IMF," J. Geophys. Res., Vol. 91, pp. 5817, 1986.

Heppner, J.P. and N.P. Maynard, "Empirical Models of High-Latitude Electric Fields," J. Geophys. Res., Vol. 82, pp. 4467-4489, 1987.

Knudsed, W.C., "Magnetospheric Convection at the High Latitude F2 Ionosphere," J. of Geophys. Res., Vol. 79, pp. 1046-1055, 1974.

Reinisch, B.W., K. Bibl, D.F. Kitrosser, G.S. Sales, J.S. Tang, Z.M. Zhang, T.W. Bullett and J.A. Ralls, "The Digisonde 256 Ionospheric Sounder," World Ionosphere/ Thermosphere Study, WITS Handbook, Vol. 2, Ed. by C.H. Liu, December 1989.

Spiro, R.W., R.A. Heelis and W.B. Hanson, "Ion Convection and the Formation of the Mid-Latitude F-region Ionization Trough," J. Geophys. Res., Vol. 83, pp. 4255-4264, 1978.

Schunk, R.W., W.J. Raitt and P.M. Banks, "Effect of Electric Fields on the Daytime High-Latitude E & F Regions," J. Geophys. Res., Vol. 80, pp. 3121-3130, 1975.

APPENDIX A

Detailed Description of the Sondrestrom DISS Upgrade

A.1 Technical Developments

A.1.1 New Drift Modes for the Digisonde 256

i) Fast Drift Modes

Ionospheric drift measurements with the Digisonde have proved very successful in the high latitude regions. The standard four antennas - four frequencies drift mode gives a minimum sample spacing of 16 × 5 msec, which corresponds to a non-aliased Doppler range of ±6.25 Hz. Horizontal ionospheric drifts often exceed 1000 ms^{-1}, at high latitudes and Doppler shifts obtained from very oblique reflection points are then too large for unambiguous resolution. New drift modes are being introduced to overcome this problem.

Since two height samples are necessary for automatic drift measurements using the ARTIST range tracking features, new modes have been introduced which always monitor two adjacent height ranges, spaced by 10 km, for each transmitted pulse. If only one frequency is monitored this speeds up the sampling rate by a factor of four, providing a non-aliased Doppler range of ±25 Hz. To keep the existing standard modes untouched with L = F for four antennas and four frequencies and/or height ranges, and L = B for all seven antennas and four frequencies and/or height ranges, the new modes with two height range sampling for each transmitter pulse use L = 0 to 7.

As indicated by Tables 1a-1d there are one and two antenna modes with one frequency only. These can be used to monitor the actual width of the Doppler spectrum up to 200 Hz (i.e. ±100 Hz) bandwidth.

The other six modes are one, two and four frequency modes for four or eight antennas each. The same modes are available with L values larger by eight for single height range sampling per transmitter pulse.

Table A-1a. Drift Data Format for N = 5 (64 Samples).

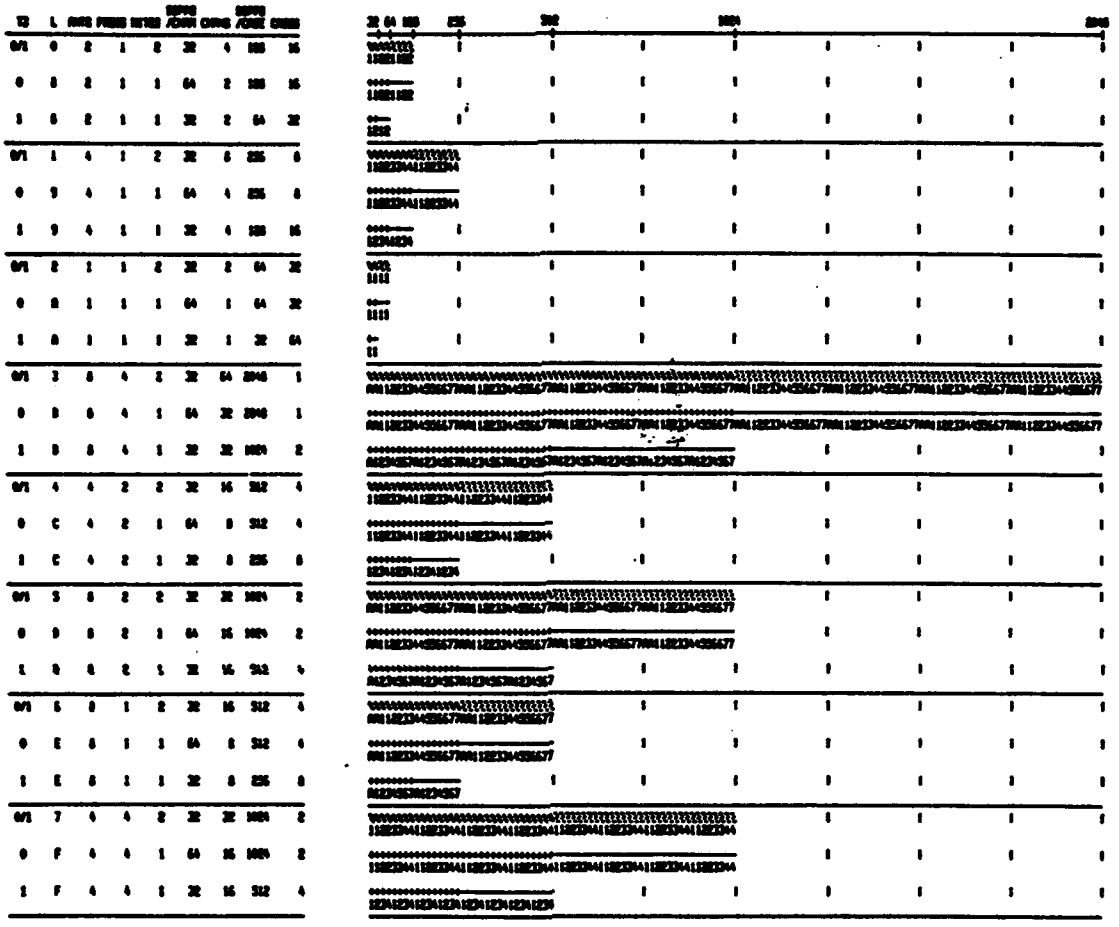

For L < 8: at each frequency, 2 height ranges ±5 km above/below the nominal height (positive Dopplers = +/+, negative Dopplers = -/-; order of data is D1 H1, D1 H2, D2 H1, . . . T3 = 0: half spectral width; T3 = 1: full spectral width, every second spectral line.

For L ≥ 8: positive Dopplers = +, negative Dopplers = -
T3 = 0: full spectral width (. . . -3/2 -1/2 +1/2 +3/2 . . .)
T3 = 1: full spectral width, every second spectral line (. . . -3 -1 +1 +3 . . .)

A = All antennas (vertical beam);
For L = 1, 4, 7, 9, C, F (4 antenna modes) replace 1, 2, 3, 4 by 1, 5, 6, 7 if Z1 = 0.

30 June 1988, CD/Bi

Table A-1b. Drift Data Format for N = 6 (128 Samples)

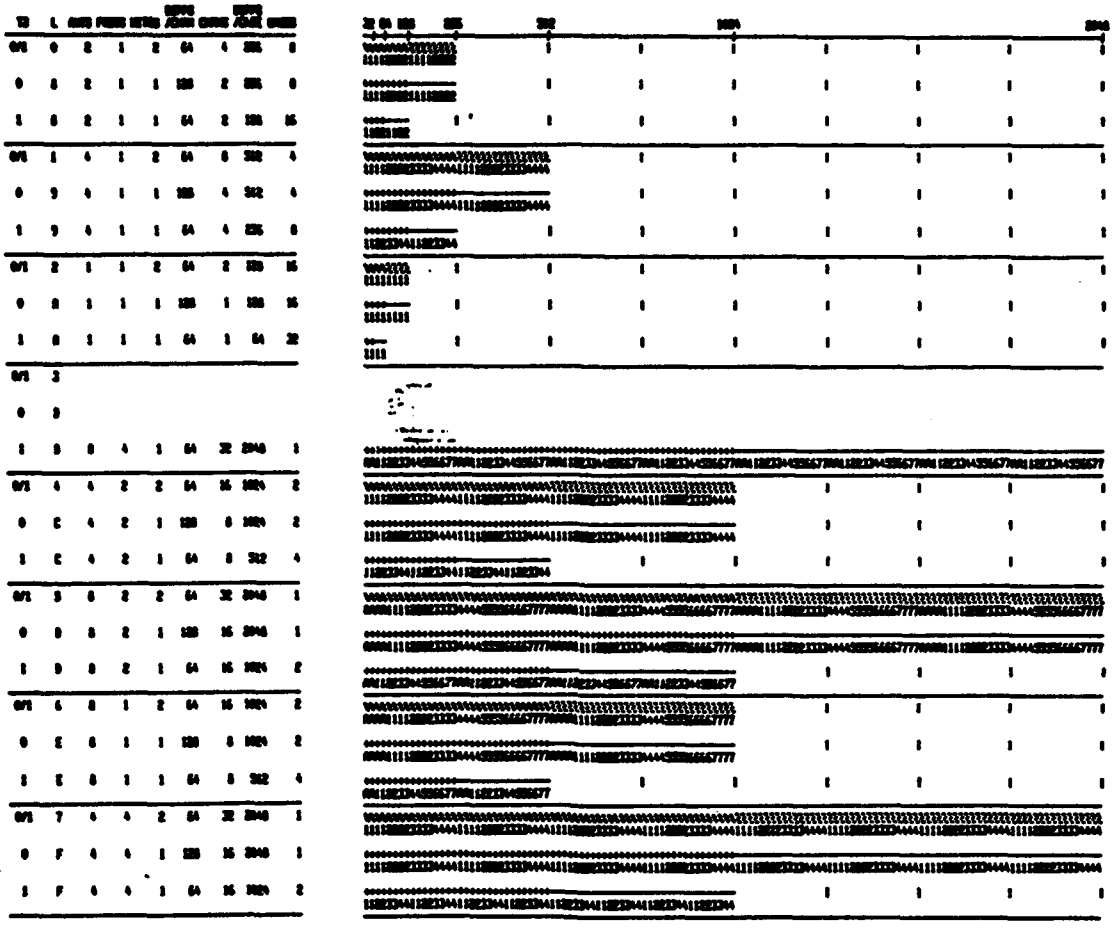

For L < 8: at each frequency, 2 height ranges ±5 km above/below the nominal height (positive Dopplers = +/+, negative Dopplers = -/-; order of data is D1 H1, D1 H2, D2 H1, . . . T3 = 0: half spectral width; T3 = 1: full spectral width, every second spectral line.

For L ≥ 8: positive Dopplers = +, negative Dopplers = -
T3 = 0: full spectral width (. . . -3/2 -1/2 +1/2 +3/2 . . .)
T3 = 1: full spectral width, every second spectral line (. . . -3 -1 +1 +3 . . .)

A = All antennas (vertical beam);
For L = 1, 4, 7, 9, C, F (4 antenna modes) replace 1, 2, 3, 4 by 1, 5, 6, 7 if Z1 = 0.

30 June 1988, CD/Bi

Table A-1c. Drift Data Format for N = 7 (256 Samples)

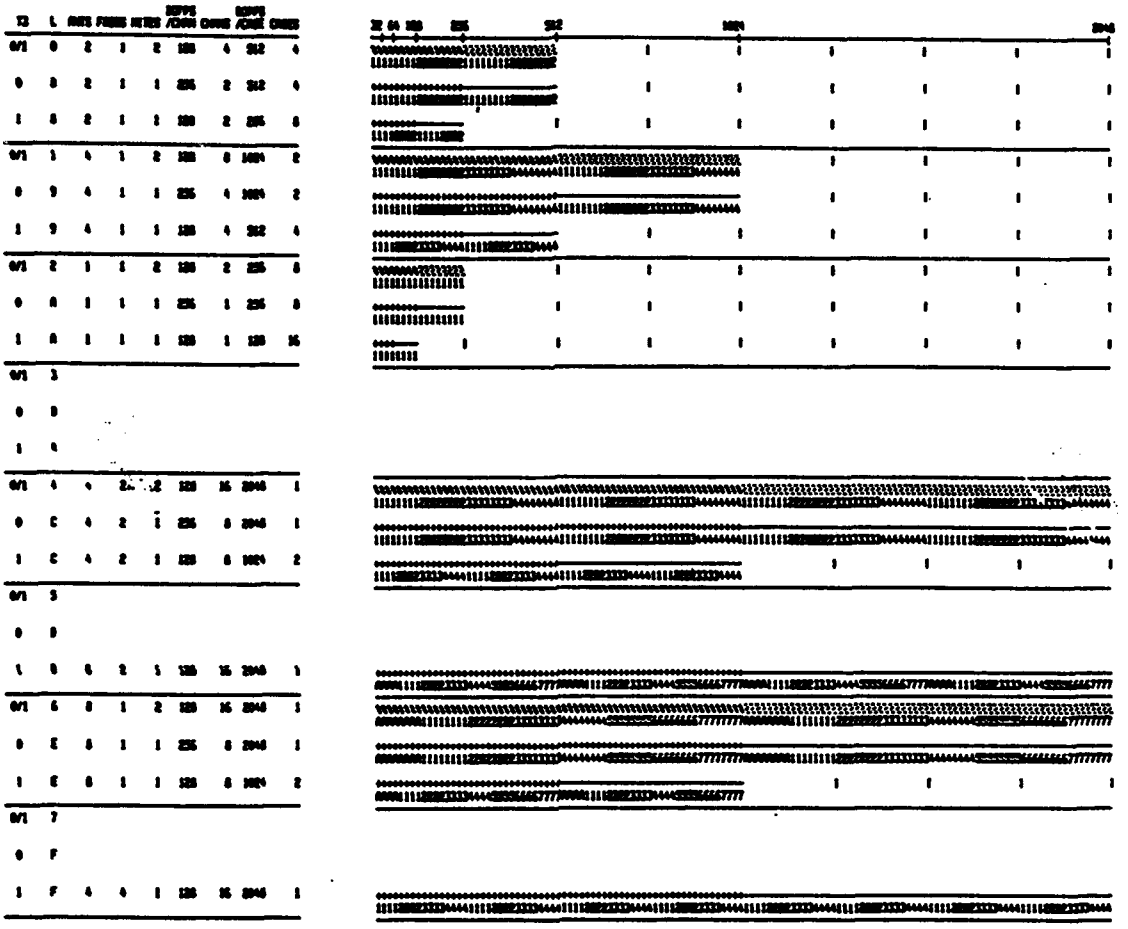

For L < 8: at each frequency, 2 height ranges ±5 km above/below the nominal height (positive Dopplers = +/+, negative Dopplers = -/-; order of data is D1 H1, D1 H2, D2 H1, . . . T3 = 0: half spectral width; T3 = 1: full spectral width, every second spectral line.

For L ≥ 8: positive Dopplers = +, negative Dopplers = -
T3 = 0: full spectral width (. . . -3/2 -1/2 +1/2 +3/2 . . .)
T3 = 1: full spectral width, every second spectral line (. . . -3 -1 +1 +3 . . .)

A = All antennas (vertical beam);
For L = 1, 4, 7, 9, C, F (4 antenna modes) replace 1, 2, 3, 4 by 1, 5, 6, 7 if Z1 = 0.

30 June 1988, CD/Bi

Table A-1d. Drift Data Format for N = 8 (512 Samples)

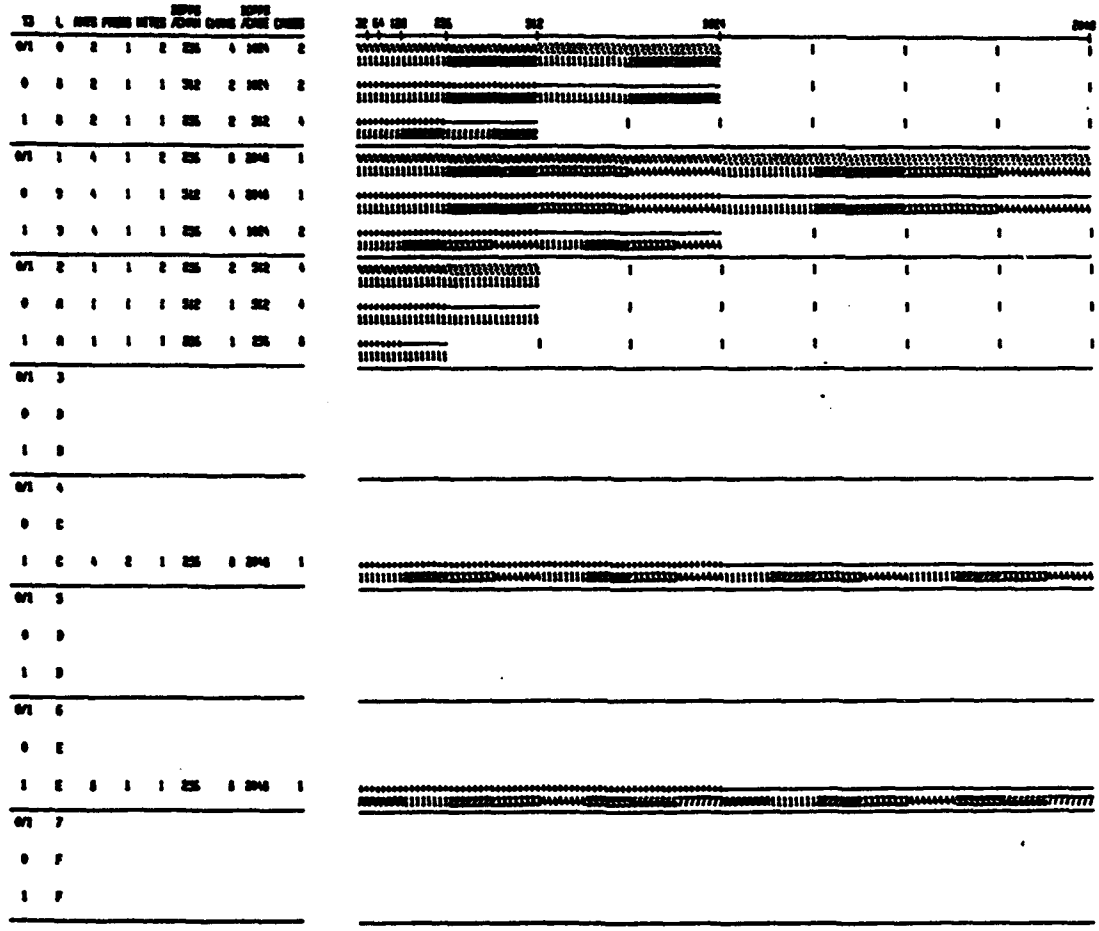

For L < 8: at each frequency, 2 height ranges ±5 km above/below the nominal height (positive Dopplers = +/+, negative Dopplers = -/-; order of data is D1 H1, D1 H2, D2 H1, . . . T3 = 0: half spectral width; T3 = 1: full spectral width, every second spectral line.

For L ≥ 8: positive Dopplers = +, negative Dopplers = -
T3 = 0: full spectral width (. . . -3/2 -1/2 +1/2 +3/2 . . .)
T3 = 1: full spectral width, every second spectral line (. . . -3 -1 +1 +3 . . .)

A = All antennas (vertical beam);
For L = 1, 4, 7, 9, C, F (4 antenna modes) replace 1, 2, 3, 4 by 1, 5, 6, 7 if Z1 = 0.

30 June 1988, CD/Bi

In the digitizer two sets of sine and cosine samples of two adjacent height ranges can be stored simultaneously. Thus it is possible to use those four data functions for multiplication with the trigonometric functions for all spectral lines. This multiplication is done in the logarithmic domain in real time by adders. The generation of those eight products require about eight microseconds. For N = 5, the Digisonde creates 64 samples on each antenna and frequency, but we produce only ±16 Doppler lines if L < 8. These 16 Doppler lines require 128 μsec of processing time after the last sampled height range. Thus only a range up to 730 km can be used for N = 5. A range up to 710 km is the limit for N = 6, 670 km for N = 7 and 590 km for N = 8 at the high repetition rate of 200 Hz.

If the storage capacity of the Integrating Memory were quadrupled, higher values of N could be used resulting in much better spectral resolution will be available for the standard modes. This enhancement would make the drift analysis at mid-latitudes more successful.

ii) 4_O - 4_X Mode

At certain times, the ionosphere is too smooth at many stations to produce enough reflection points in the skymaps for a meaningful drift analysis. For those cases the eight-antenna mode has been extended to use four antennas with ordinary and with extraordinary polarization, thus doubling the number of sources. The possibilities which are specifically useful for stations which have only four antennas are described in Table 2.

This feature was first used for calibration of the antenna field. In this situation only the reference signal fed directly into one antenna input of the Antenna Switch and the signal arriving from one pre-amplifier box provide useful data. However, if P2 = 7 and P3 = 0 is chosen and the antenna 1 input is selected to be connected to the

L	Z	F1	F2	F3	F4
	0	1o 5o 6o 7o 1x 5x 6x 7x	Same	Same	Same
	1	1o 2o 3o 4o 1x 2x 3x 4x	Same	Same	Same
	2	Allo 1o 2o 3o 4o 5o 6o 7o	Same	Same	Same
B*	3	1x 5x 6x 7x 1x 5x 6x 7x	Same	Same	Same
	4	1o 5o 6o 7o 1o 5o 6o 7o	Same	1x 5x 6x 7x 1x 5x 6x 7x	Same
	5	1o 2o 3o 4o 1o 2o 3o 4o	Same	1x 2x 3x 4x 1x 2x 3x 4x	Same
	6	Allo 1o 2o 3o 4o 5o 6o 7o	Same	Allx 1x 2x 3x 4x 5x 6x 7x	Same
	7	1o 2o 3o 4o 1o 5o 6o 7o	Same	1x 2x 3x 4x 1x 5x 6x 7x	Same

		F1	F2	F3	F4
*	0	1o 5o 6o 7o	Same	Same	Same
*	1	1o 2o 3o 4o	Same	Same	Same
	2	Allo 1o 2o 3o	Same	Same	Same
F	3	1x 5x 6x 7x	Same	Same	Same
	4	1o 5o 6o 7o	Same	1x 5x 6x 7x	Same
	5	1o 2o 3o 4o	Same	1x 2x 3x 4x	Same
	6	Allo 1o 2o 3o	Same	Allx 1x 2x 3x	Same
	7	1x 2x 3x 4x	Same	Same	Same

STANDARD DRIFT MODES*

AND EXTENSIONS TO

MEASURE X-COMPONENT

Bi 15 Feb 89

Table A-2. Possibilities for Four Antenna Stations

eight reference signal, and L = B and Z = 9 then the pre-amplifier boxes 2, 3, and 4 can be monitored sequentially. As Table 3 indicates, all phase bits of the spectral lines are displayed simultaneously while the maximum amplitude is indicated as the printer gain in the last column on the left.

If Z = 8 is chosen the outer antenna boxes 5, 6, and 7 can be monitored sequentially as a function of frequency. For each frequency the indicated phases should be almost the same for each of the tested antennas. But there should be a phase shift of 90° between the second and sixth line for antennas 2 (or 5) or between the third and seventh line for antennas 3 (or 6) or between the fourth and eighth line for antennas 4 (or 7).

Table 3 shows all the options for raw spectral data readout using the processor printer output port. This table includes new and standard Drift modes, controlled by "L," "N," and "T3." The format of the printed data, which is only a subset of the recorded data, is controlled by P2, P3, and P6.

A.1.2 Direct Communication

As originally designed, the Input Computer (INCPU) of the Digisonde 256 Processor was optimized for receiving instructions or input from a human typing at normal rates of speeds. As the ARTIST and the AUTODRIFT schemes have developed, it has become desirable for the IBM PC/AT computer which is attached to the Processor chassis to supply instructions to the Pprocessor as result of computer decisions.

The control of the Processor chassis hardware by the INCPU is performed in a interrupt service routine triggered by a 1/8 second clock. This interrupt service routine takes 40 to 50 milliseconds to perform its tasks and if more than one input character arrives at the INCPU serial port

Table A-3. Prinout for New Drift Modes

P2		Left	Right	Type of Phase
0	No Print			
1	All freq./hts.	Amplitude	4 MSB Phase	Absolute
2	All freq./hts.	Amplitude	4 Middle Bits	Absolute
3	No Print			
4	All Cases	Amplitude	4 MSB Phase	Absolute
5	All Antennas	Amplitude	4 MSB Phase	Relative
6	All Antennas	Amplitude	4 Middle Bits	Relative
7	All Antennas	4 MSB Phase	4 LSB Phase	Relative

Add 8 to Compress ±64 or ±32 Doppler cases. Skip every other Doppler. If the ±64 Doppler case is not compressed, then only the inner Doppler lines will be printed.

P3 = Ant. No., 0, 1, 2, 3 or 0, 1, 2, 3, 4, 5, 6, 7. Add 8 to send data to ARTIST.

P6 = Freq. No., 0 or 0, 1 or 0, 1, 2, 3. Add 8 to look at 2nd Height range is 2nd Height range wasn't printed on same line as 1st Height range, i.e. if FHpLn = 1 and NHts >=2.

Format when there are ±32 Dopplers or uncompressed ±64 Dopplers:

```
**************Left**************     **************Right**************
-31              -1 +1              +31 -31              -1 +1              +31
```

Format for compressed ±64 Dopplers (odd spectra only):

```
**************Left**************     **************Right**************
-61              -1 +1              +61 -61              -1 +1              +61
```

Format for ±16 Dopplers or compressed ±32 Dopplers:

```
**************Left**************     **************Right**************
******F/H1******    ******F/H2******    ******F/H1******    ******F/H2******
-15    -1 +1    +15 -15    -1 +1    +15 -15    -1 +1    +15 -15    -1 +1    +15
```

Format for ±16 Dopplers and only one freq./height:

```
        *******Left*******                  *******Right*******
-16      -1 +1      +16                -16      -1 +1      +16
```

DpTbl:

	L	N	T3	NFreq	NAnt	NSpec	NHts	NCase	ModNSpec P2 = 0,8		FHpLN P2 = 0,8		SpecInc P2 = 8
Db	1,	5,	0, 4	1,	4,	16,	2,	8,	16,	16,	2,	2,	1
Db	1,	6,	0, 4	1,	4,	32,	2,	4,	32,	31,	1,	2,	2
Db	3,	5,	0, 4	4,	8,	16,	2,	1,	16,	16,	2,	2,	1
Db	4,	5,	0, 4	2,	4,	16,	2,	4,	16,	16,	2,	2,	2
Db	4,	6,	0, 4	2,	4,	32,	2,	2,	32,	31,	1,	2,	2
Db	9,	5,	0,	1,	4,	16,	1,	16,	32,	32,	0,	0,	1
Db	9,	6,	0,	1,	4,	32,	1,	8,	32,	32,	1,	1,	1
Db	9,	6,	4,	1,	4,	16,	1,	16,	32,	32,	0,	0,	1
Db	9,	7,	4,	1,	4,	32,	1,	8,	32,	32,	1,	1,	1
Db	12,	5,	0,	2,	4,	16,	1,	8,	16,	16,	2,	2,	1
Db	12,	6,	0,	2,	4,	32,	1,	4,	32,	31,	1,	2,	2
Db	12,	6,	4,	2,	4,	16,	1,	8,	16,	16,	2,	2,	1
Db	12,	7,	4,	2,	4,	32,	1,	4,	32,	31,	1,	2,	2
Db	15,	6,	0,	4,	4,	64,	1,	1,	32,	63,	1,	1,	2
Db	15,	5,	0,	4,	4,	32,	1,	2,	32,	31,	1,	2,	2
Db	15,	6,	4,	4,	4,	32,	1,	2,	32,	31,	1,	2,	2
Db	11,	5,	0,	4,	8,	32,	1,	1,	32,	31,	1,	2,	2; Default

during this time it will be lost. This was not a problem for a human typist but required direct communication from the IBM computer to be sending characters with long delays between characters rather than sending at the 240 characters per second (2400 baud) permitted by other hardware/ software constraints.

Strategically, it is also more efficient to put data directly into specified INCPU memory locations and to read data also directly from INCPU memory locations without all of the overhead required for "user friendly" human I/O.

The DIRECT communication scheme which was developed allows high level (Fortran) programs running in the IBM PC/AT computer to send or receive strings of data directly to or from specified INCPU memory locations at 2400 baud.
The following elements of the Digisonde 256 were modified:

Card 01 of the Processor has an unused inverter in a 74LS04 connected between a card edge pin and the "Data Ready" pin of the 8251 USART.

A wire is added under the chassis connecting the Data Ready signal from the card 01 8251 USART to card 02 level 6.5 interrupt which was already available on the card 02 edge connector.

The card 02 (INCPU) firmware module DGS256 was modified by removal of the data input coding. All data input to DGS256 is now done by calling a subroutine in another INCPU module, MONINP, which polls a circular buffer. MONINP has added an interrupt handler which puts inputted characters into a circular buffer. Polled input, performed when the INCPU is idle between the 1/8 second interrupts for controlling the processor hardware, also puts data into the circular buffer. The retention of polled input capability was done to permit the same firmware to be used on Digisonde 256 Processors which do not have the hardware modification to card 01 and the wire added to the chassis.

The DGS256 module also has added procedures to act upon special 8 bit (as opposed to normal 7 bit ASCII) strings for stuffing up to 16 bytes, or nibbles, into an address (embedded in the string). The strings require only 19 characters to transfer 16 bytes or 11 characters to transfer 16 nibbles. A command string of 3 characters is required for a read instruction. Data read from the INCPU memory is sent to the IBM PC/AT computer using the addressed output intended for the window in the upper left of the screen except the address used is 64 rather than the 0 to 63 for the 64 locations of the window. Worst case times for reading of 16 bytes is 110 milliseconds; for 16 nibbles it is 75 milliseconds.

There is also a mode for sending a word command directly to the INCPU input buffer such as RUN A1, etc. and a mode for testing the commands by a human typing ASCII hexadecimal numbers at the console to emulate 8 bit numbers. The firmware source listing contains examples and full instructions. See Appendix B.

The ARTIST module DGSTERM (a Terminate and Stay Resident, TSR utility which is responsible for the processor terminal function of the ARTIST computer) was modified to assemble the strings required for the direct communication to the processor chassis (see Appendix C). The same software interrupt used by other programs interacting with DGSTERM had 5 new subfunctions added so that a calling program need only to put the INCPU address in the AX register, a count in the CX register, a PC address in the BX register and then call the appropriate subfunction to effect the transfer. A scheme is also included for flagging the successful completion of a Read command.

Test routines were added at the end of the DGSTERM program as examples to base routines in calling programs on and to permit testing all of the subfunctions by executing the test routines with a software debugger.

The software interrupt functions in DGSTERM are convenient for other assembly language routines to access, but to allow convenient access from Fortran programs an assembly language subroutine named DIRECT was written in a style which allows it to be called from a Fortran program with

the standard high level language argument passing convention (see Appendix D). This routine, when linked to a Fortran program, can be called from a Fortran program with Fortran variables as arguments. The functions in DIRECT include subroutines for writing strings of bytes or nibbles to the INCPU memory, reading bytes or nibbles from the INCPU memory, sending commands to the INCPU, reading or writing 2 byte Fortran integers from or into one to five BCD INCPU memory locations, and reading or writing all 32 memory locations of the INCPU Drift parameter buffer (4 frequencies, 4 heights, and 4 gains).

A Fortran program, TESTDIR (see Appendix E), was written to illustrate proper usage of the subroutines in the module DIRECT. Also the execution of TESTDIR exercises all of the direct communication procedures and will confirm that all of the above described software and hardware modifications are installed properly.

Presently, this new Direct communication feature is being used by AUTODRIFT. In the near future the TIME TRANSFER procedure in ARTIST will make use of it also. Eventually it is envisioned to use Direct communication when altering Ionogram parameters in response to ARTIST scaling results.